

Lawrence Berkeley National Laboratory

Recent Work

Title

A MODEL FOR PREDICTING AIR FLOWS THROUGH TWO COMBUSTION APPLIANCES VENTED BY A SINGLE CHIMNEY

Permalink

<https://escholarship.org/uc/item/11q848h4>

Authors

Dumortier, D.
Modera, M.P.

Publication Date

1987-10-01

UC-95d
LBL-23151
c.1



Lawrence Berkeley Laboratory

UNIVERSITY OF CALIFORNIA

APPLIED SCIENCE DIVISION

RECEIVED
LAWRENCE
BERKELEY LABORATORY

JAN 3 1989

LIBRARY AND
DOCUMENTS SECTION

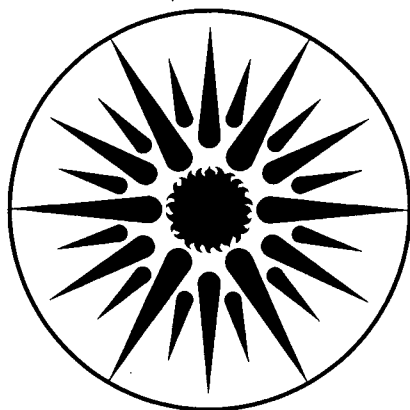
A Model for Predicting Air Flows through Two Combustion Appliances Vented by a Single Chimney

D. Dumortier and M.P. Modera

October 1987

For Reference

Not to be taken from this room



APPLIED SCIENCE
DIVISION

LBL-23151
c.1

DISCLAIMER

This document was prepared as an account of work sponsored by the United States Government. While this document is believed to contain correct information, neither the United States Government nor any agency thereof, nor the Regents of the University of California, nor any of their employees, makes any warranty, express or implied, or assumes any legal responsibility for the accuracy, completeness, or usefulness of any information, apparatus, product, or process disclosed, or represents that its use would not infringe privately owned rights. Reference herein to any specific commercial product, process, or service by its trade name, trademark, manufacturer, or otherwise, does not necessarily constitute or imply its endorsement, recommendation, or favoring by the United States Government or any agency thereof, or the Regents of the University of California. The views and opinions of authors expressed herein do not necessarily state or reflect those of the United States Government or any agency thereof or the Regents of the University of California.

LBL-23151

A MODEL FOR PREDICTING AIR FLOWS THROUGH
TWO COMBUSTION APPLIANCES VENTED BY A SINGLE CHIMNEY

Dominique Dumortier, Mark P. Modera
Applied Science Division
Lawrence Berkeley Laboratory
1 Cyclotron Road
Berkeley, California 94720

October 1987

This work was funded under contract to the Department of the Army and supported by the Assistant Secretary for Conservation and Renewable Energy, Office of Building Energy Research and Development, Building Systems Division of the U.S. Department of Energy under Contract No. DE-AC03-76SF00098.

A MODEL FOR PREDICTING AIR FLOWS THROUGH TWO COMBUSTION APPLIANCES VENTED BY A SINGLE CHIMNEY

Dominique Dumortier, Mark P. Modera

Energy Performance of Buildings Group
Applied Science Division
Lawrence Berkeley Laboratory
University of California
Berkeley, California 94720

October 1987

ABSTRACT

This report describes the development of a computer program that predicts air flows and temperatures in a chimney venting two combustion appliances. Mass conservation, energy conservation and pressure loss equations are used in conjunction with a thermal model of a chimney to define the system. The resulting system of 18 equations and 18 unknowns is reduced to a single equation, which is then solved by a numerical method. Although the model is generally applicable to venting systems serving two combustion appliances, the case which is examined in detail is that of a steam boiler and domestic hot water heater (DHW) connected to a common masonry chimney in a multifamily building. This installation is typical of those encountered in turn-of-the-century construction in midwestern and northeastern U.S. cities. The computations required to determine the leakage areas of each of the components of the venting system are described, as is a preliminary examination of the model performed by comparing air flow and temperature predictions with measured values for the multifamily boiler-DHW system. The comparison showed good agreement between predictions and experimental results, however a more thorough evaluation of model predictions for systems with and without vent dampers would be appropriate.

TABLE OF CONTENTS

INTRODUCTION	page: 6
FLOW MODEL	page: 8
DYNAMIC THERMAL MODELS	page:15
SOLUTION OF THE SYSTEM OF EQUATIONS	page:21
COMPARISON WITH MEASURED DATA	page:27
FUTURE WORK	page:28
APPENDIX A: EFFECTS OF GAS COMPOSITION VARIATION	page:40
APPENDIX B: LEAKAGE AREA COMPUTATION TECHNIQUES	page:42
APPENDIX C: REDUCTION OF THE SYSTEM OF EQUATIONS	page:65
APPENDIX D: INPUT AND OUTPUT DATA FOR 8-UNIT APARTMENT BUILDING	page:71

NOMENCLATURE

SYMBOLS:

A	cross sectional area of a duct [m^2],
C_l	leakage area coefficient [dimensionless],
C_p	heat capacity [$\text{J}/(\text{kg K})$],
D	hydraulic diameter, defined as four times the ratio of the cross sectional area to the section perimeter [m],
d	characteristic inside dimension of the chimney [m],
$dA_{i,n}$	area of an element of the inside surface of the chimney [m^2],
$dA_{o,n}$	area of an element of the outside surface of the chimney [m^2],
dV	volume of an element of the chimney walls [m^3],
E	stack induced pressure [Pa],
e	thickness of the chimney walls [m],
f	friction factor [dimensionless],
g	acceleration of gravity [9.81 m/s^2],
Gr_d	Grashof number corresponding to a length l of heat transfer surface [dimensionless],
\bar{h}_c	convective heat transfer coefficient [$\text{W}/(\text{m}^2 \text{ K})$],
\bar{h}_r	radiative heat transfer coefficient [$\text{W}/(\text{m}^2 \text{ K})$],
$\bar{h}_{i,n}$	overall heat transfer coefficient for inside of chimney [$\text{W}/(\text{m}^2 \text{ K})$],
$\bar{h}_{o,n}$	overall heat transfer coefficient for outside of chimney [$\text{W}/(\text{m}^2 \text{ K})$],
h_b	stack height of the boiler [m],
h_d	stack height of the DHW heater [m],
h_s	stack height of the chimney [m],
k	thermal conductivity [$\text{W}/(\text{m K})$],
K	dynamic pressure loss coefficient (C_o in ASHRAE Handbook) [dimensionless],
K'	dimensional constant in simplified expression for free convective heat transfer coefficient [$15.9 \text{ W}/\text{m}^2 \text{ K}^{0.92}$],
l	length of a duct [m],
L	leakage area [m^2],

m	mass flow rate [kg/s],
M_b	a function which depends only on the mass flowrate through the boiler [kg/s],
P	air pressure [Pa],
Pr	Prandtl number [dimensionless],
p	average perimeter of the chimney, $(p_{\text{inside}} + p_{\text{outside}})/2$ [m],
Q	rate of energy input to a combustion appliance [W],
Q_t	rate of energy input to the air flowing through a combustion appliance [W],
R	flow resistance [$\text{kg}^{-1} \text{m}^{-1}$],
R_U	ratio of conductance-area product outside the chimney mass to conductance-area product inside the mass [dimensionless],
Re	Reynolds number [dimensionless],
t	time elapsed since the beginning of a combustion-appliance cycle [s],
T	temperature [K],
T_{ref}	reference temperature [273.16 K],
U_{in}	total thermal conductance inside chimney mass [$\text{W}/\text{m}^2\text{K}$],
U_{out}	total thermal conductance outside chimney mass [$\text{W}/\text{m}^2\text{K}$],
v	air velocity inside a duct [m/s],
z	height of a point inside the chimney [m].

GREEK SYMBOLS

β	coefficient of volume expansion for air [K^{-1}]
ΔP	pressure change in the flow stream [Pa],
$\Delta \rho$	density difference [Pa],
Δt	simulation timestep [s],
Δz	height-step in chimney heat transfer model [m],
ϵ	roughness height [m],
ϵ_b	boiler draft diverter flow direction indicator [dimensionless],
ϵ_d	DHW draft diverter flow direction indicator [dimensionless],
λ_z	length-based chimney constant [m],

λ_t	time-based chimney constant [s],
η	combustion appliance efficiency [dimensionless],
ν	kinematic viscosity [m^2/s],
ρ	density [kg/m^3],
ρ_{ref}	reference air density at T_{ref} [$1.29 \text{ kg}/\text{m}^3$],
τ_{fire}	short time constant of a component of a combustion appliance system [s],
$\tau_{standby}$	long time constant of a component of a combustion appliance system [s],

SUBSCRIPTS

air	stands for air stream,
amb	stands for ambient air surrounding chimney,
b	stands for boiler,
bd	stands for boiler draft diverter,
br	stands for boiler room,
brick	stands for chimney brick,
bs	stands for boiler stack,
c	stands for local chimney air,
cb	stands for chimney bottom,
cm	stands for chimney mean,
d	stands for domestic hot water (DHW),
dd	stands for DHW draft diverter,
ds	stands for DHW stack,
entr	stands for the entrance of a duct,
eqv	stands for equivalent,
exit	stands for the exit of a duct,
out	stands for outside air,
s	stands for total (chimney) stack,
surface	stands for chimney surface,
water	stands for the water in either the boiler or DHW heater,

INTRODUCTION

Multifamily buildings are approximately one quarter of the U. S. housing stock, consume over two quads of energy per year, and represent a considerable potential for energy conservation. This report represents part of a research effort initiated in 1983 to evaluate existing alternatives and develop new alternatives for retrofitting multifamily buildings to reduce energy consumption.¹ The objective of the work described in this report was to develop a tool for evaluating the energy savings associated with installing vent dampers in combined boiler/domestic-hot-water systems.

In 1983, a Lawrence Berkeley Laboratory (LBL) research team developed and tested a set of diagnostic techniques to examine retrofits in a multifamily building.² One of the retrofits examined was a vent damper, a retrofit that restricts the air flow through the boiler stack when the boiler is not operating. The energy savings that could be attributed to this retrofit was estimated by measuring the instantaneous off-cycle heat loss up the boiler stack with and without the vent damper. This was accomplished by measuring the flow rate (with a tracer gas) and temperature of the air in the boiler stack. These measurements showed that the addition of a vent damper should reduce the energy consumption of the boiler by approximately 10%.

The substantial savings attributed to the vent damper — which agreed with the savings measured by flip-flop measurements in the same building — drew the attention of researchers, energy service companies, and government energy agencies.³ However, flip-flop experiments in similar buildings showed significant variations in the energy savings that could be attributed to vent dampers.⁴ This report describes the development of an analytical model of combustion appliances that takes into account the principal factors affecting the energy savings to be expected with a vent damper.

A search of the literature uncovered a number of models for predicting air flow through chimneys and combustion appliance vents.^{5,6} One program treats the flow through a residential furnace in great detail, such that it can predict spillage (flow from the heating system flue into the house), and backdrafting (flow down the chimney into the room).⁷ However, the existing programs could not be applied to multifamily buildings because they do not treat the case of multiple combustion appliances connected to a single chimney. A large number of multifamily buildings either have two separate heating appliances, or a heating appliance and a domestic hot water heater, connected to the same chimney. Thus, our model had to take into the interaction of two separately-controlled combustion appliances.

An additional criteria in the development of our program was that a user of the program should be able to obtain the inputs either by physical examination of the system, or by easily-performed diagnostic measurements.

Typical Boiler, Water Heater and Chimney Configuration

Multifamily buildings built in midwestern cities around the turn of the century typically utilize a gas fired, single-pipe steam boiler and a gas-fired Domestic Hot Water (DHW) heater connected via ductwork to a single chimney. Most of the steam heating systems were originally coal-fired, some of which were converted to natural gas, the remainder having been replaced completely by gas-fired boilers. In almost all cases, the boiler, and very often the DHW heater, are vented through the original chimney built for coal firing. Neither the boiler nor DHW heater are connected directly to the chimney, but rather are connected via draft diverter systems. Draft diverters serve two purposes. They reduce the variability in flow rate through the combustion appliance that would be induced by changes in chimney or ambient temperatures, and they dilute the combustion-product gasses with relatively dry air to reduce the possibility of condensation inside the chimney. Thus, the flow through the combustion appliance is controlled by its temperature, whereas variations in the chimney temperature result in increased flows from the boiler room up the chimney.

In practice, a draft diverter simply consists of an opening from the boiler or DHW heater ductwork to the boiler room. Combustion products leaving the boiler or DHW flue are mixed with boiler-room air at the draft diverter. Some buildings use barometric dampers rather than draft diverters. The difference between a barometric damper and a draft diverter is that a barometric damper restricts the opening between the stack and the boiler room when the boiler is not firing. The damper is opened during firing by the increased pressure drop across the damper.

Another potential component of these heating systems, a vent damper, reduces the flow through the boiler or DHW ductwork when they are not firing. These dampers usually consist of butterfly valves located in the ductwork downstream of the draft diverter and upstream of the chimney entry. There are two common types dampers: 1) spring-loaded dampers that are closed by an electric motors controlled by the thermostat activation signal, and 2) bimetallic dampers which are open or closed depending upon the temperature in the ductwork.

FLOW MODEL

Flow path description

The model described in this report can be used to predict the flows through all components of a two-combustion-appliance system vented through a common chimney. The flow path used in the model is illustrated in Figure 1. The major components of the system are: the boiler, the DHW heater, the boiler draft diverter, the DHW heater draft diverter, the boiler stack (the boiler vent ductwork after the draft diverter), the DHW heater stack (the DHW vent ductwork after the draft diverter), and the chimney.

The major component missing from Figure 1 is the basement envelope, which connects to outside and to the building above. We assume that the boiler room air is entering the system solely through the boiler room walls. Although boiler room air can be drawn from the building above, modeling the flow through a multistory building is a complex problem in and of itself, and was considered to be beyond the scope of this study.⁸ However, the boiler rooms in most of these buildings have a large number of leaks to outside, in some cases intentional leaks specifically designed to provide combustion and make-up air. In addition, the stack effect of the building inhibits the air flow from the building to the boiler room. Both these factors reduce the effect of the building on the combustion-system air flow.

Model Assumptions

A number of assumptions were made in the development of the model. In general, these assumptions were made to reduce the complexity associated with exact modeling of the air-flow and heat transfer processes occurring in the venting system. On the other hand, the model was kept general with respect to the types of physical configurations that it can simulate (i.e. simplifications based upon expected system configurations were avoided whenever possible).

• Gas Temperatures

For the purpose of computing stack effects, temperatures are assumed to be homogeneous in the boiler room and in all components of the heating system except the chimney. These temperatures are determined from the average temperature in each component. This approximation is based upon the relatively small vertical dimensions of the boiler, boiler stack, DHW heater and DHW stack compared to the length of the chimney. In a component such as the boiler or DHW heater, which has a large temperature rise between the entrance and the exit, the pressure drops through the entrances and exits are based upon the gas temperature of the entering or exiting air. In the chimney, the temperature is taken as homogeneous at each cross section,

however it changes along the length of the stack. In the following, we will characterize the temperature inside the chimney by two temperatures: the temperature at the bottom of the chimney and the mean temperature inside the chimney. The unknown temperatures are then:

- T_b Temperature of the boiler.
- T_d Temperature of the DHW heater.
- T_{bs} Temperature of the boiler stack.
- T_{ds} Temperature of the DHW stack.
- T_{cb} Temperature of the chimney bottom.
- T_{cm} Mean temperature inside the chimney.

• Pressures

The pressure is assumed to be homogeneous in the boiler room, except for the computation of the stack effect in the boiler and the DHW heater. The pressure is also assumed to be homogeneous at each cross section of the different components of the heating system. The outside pressure at the boiler room level is taken as the pressure reference.

• Density Calculations

During combustion appliance operation the composition of the gasses passing through the system changes along the flow path due to the combustion of CH_4 , which combines with O_2 to produce CO_2 and H_2O according to the following process:



In principle, density calculations should take into account the fact that the gas composition varies. However, calculations presented in Appendix A show that the difference between the density of the flow considered as a gas mixture and the density of the flow considered as pure air, is less than 6%. Thus, we neglected the fact that the flow was a mixture of air and combustion products for all density calculations. The gas density ρ (kg/m^3) is computed as a function of temperature according to the following formula:

$$\rho = \rho_{ref} \frac{T_{ref}}{T} \quad [2]$$

- **Flow Regime**

Based upon measurements of flows in a typical venting system, we derived the Reynolds number corresponding to the flow through each component, where:

$$Re = \frac{v D}{\nu} \quad [3]$$

For the case where the boiler was not being fired and the DHW heater was cycling, the computed Reynolds numbers indicated turbulent flows $Re \geq 2000$ in all components after the boiler and DHW heater exits. When either the boiler or DHW heater were being fired, the flows through the heaters themselves became turbulent, whereas during the off-cycle they were in the transition regime.

For turbulent flow, the Darcy-Weisbach relation can be used to describe the frictional pressure losses:

$$\Delta P = \frac{\rho f l v^2}{2 D} \quad [4]$$

As entrance and exit losses are also proportional to the square of the flowrate in all flow regimes, we assume that pressure losses throughout the system are proportional to the square of the flowrate.

Theoretical Basis of the Model

- **Conservation of mass**

In a system without mass generation, the mass entering the system is equal to the mass leaving the system.

- **Conservation of energy**

The energy input to a component plus the energy generated in that component is equal to the energy that leaves the component.

- **Fluid Dynamics**

The pressures driving the air flows in the system are created by stack effects due to temperature differences between the different components of the system. The pressure losses in the system result from either frictional or dynamic losses.

In a component containing a fluid whose density is not equal to that of its surroundings, there will be pressure differences between the gas in that component and the surrounding gasses. These pressure differences, which drive the flow through the sys-

tem, can be expressed as:⁹

$$\Delta P_s = \Delta \rho g (z_{exit} - z_{entr}) \quad [5]$$

The pressure losses induced by frictional losses are expressed in Equation 4 as a function of the velocity squared (which is equivalent to the flowrate squared).

Dynamic pressure losses correspond to kinetic energy losses, and also are related to the square of the velocity:

$$\Delta P = \frac{\rho K v^2}{2} \quad [6]$$

Flow Resistance Formalism

The pressure loss characteristics of a given component due to frictional losses and dynamic losses are expressed using the leakage area formalism. This is the formalism conventionally used to characterize the flow characteristics of building envelopes. The leakage area can be thought of as an effective flow area, analogous to a conductance that relates the flowrate to the square root of the pressure drop.

First, consider the expression for the pressure drop due to frictional losses:

$$\Delta P = \frac{\rho f l v^2}{2 D} \quad [4]$$

By expressing the velocity v in terms of the mass flow rate, m :

$$v = \frac{m}{\rho A} \quad [7]$$

and substituting this expression into Equation 4, the pressure difference expression becomes:

$$\Delta P = \frac{\rho f l}{2 D} \left(\frac{m}{\rho A} \right)^2 \quad [8]$$

Introducing the leakage area formalism, we obtain a general expression for the pressure difference due to frictional losses inside a duct:

$$\Delta P = \frac{m^2}{2 \rho L^2} \quad [9]$$

with the leakage area defined as:

$$L = C_l A \quad [10]$$

and

$$C_l = \sqrt{\frac{D}{f l}} \quad [11]$$

Substituting the leakage area into the expression for the pressure drop due to dynamic losses, we obtain the same result with a different leakage area coefficient:

$$C_l = \frac{1}{\sqrt{K}} \quad [12]$$

All pressure drops in the system can now be expressed using Equation 9. The total pressure drop due to frictional losses, dynamic losses and stack effect is then:

$$\Delta P = -\Delta P_s + \frac{1}{2 \rho} \left(\frac{m}{L}\right)^2 \quad [13]$$

Leakage areas can be calculated from tables given in the ASHRAE Handbook of Fundamentals.¹⁰ The major difficulty is to match the actual configurations with the simplified cases presented in ASHRAE. Appendix B demonstrates techniques for combining leakage area coefficients in series or in parallel, and presents the results for a typical venting system.

Network Representation of the Flows

Utilizing the flow path and assumptions described above, a network representation of the venting system can be made. Figure 2 is a representation of this network using electrical network notation. In this figure, inverse leakage areas are represented as resistors, and stack-effect driving pressures are represented as voltage sources. However, although electrical network symbolism provides a convenient representation of the flows and pressures throughout the system, it should be noted that the pressure drops across the resistors are proportional to the mass flow rate squared. Thus, the equations for combining resistances in series and parallel must be redefined (see Appendix B).

In Figure 2, the boiler and DHW heater represent symmetric halves of the network. Stack effect is simulated for the boiler flue, the DHW flue and the chimney. Stack effect is not simulated for draft diverters and stacks due to the small vertical rises in these components. Resistances in the network are obtained from the component leakage areas.

Model Derivation

From the network in Figure 2 we can derive mass and energy balance equations for each node:

• Conservation of Mass

$$m_{bs} = m_b + m_{bd} \quad [14]$$

$$m_{ds} = m_d + m_{dd} \quad [15]$$

$$m_s = m_{bs} + m_{ds} \quad [16]$$

Throughout the model development, the contribution of natural gas to the mass flow through the boiler or DHW heater during firing is not treated explicitly. This flow appears in the total air flow through the appliance, and therefore should be subtracted from the computed flows to determine the air flow. However, as we are assuming that the natural gas follows the same path as the air through the appliance, because the natural gas is not submitted to the entrance pressure loss, the computed pressure losses through the appliances will be somewhat high. Analysis of the individual contributions to the appliance pressure losses (Appendix B) while taking into account relative flowrates of natural gas and air shows this effect to be negligible. Also, as we are assuming that the mass flowing through the system comes only from the boiler room, the mass leaving the system through the chimney is equal to the mass entering the system through the boiler room:

$$m_{br} = m_s \quad [17]$$

• Conservation of energy

$$m_b C_{p_{air}} (T_b - T_{br}) = Q_{lb} \quad [18]$$

$$m_d C_{p_{air}} (T_d - T_{br}) = Q_{ld} \quad [19]$$

$$m_{bs} T_{bs} = m_b T_b + m_{bd} T_{br} \quad [20]$$

$$m_{ds} T_{ds} = m_d T_d + m_{dd} T_{br} \quad [21]$$

$$m_s T_{cs} = m_{bs} T_{bs} + m_{ds} T_{ds} \quad [22]$$

In Equations 18 and 19, Q_{lb} and Q_{ld} are the energy input to the air streams through the boiler and DHW heater, respectively. Both of these parameters are time-dependent, the profiles for which will be derived below.

• Pressure drops

$$P_{out} - P_{br} = \frac{1}{2\rho_{out}} \left(\frac{m_{br}}{L_{br}} \right)^2 \quad [23]$$

$$P_{br} - P_b = \frac{1}{2\rho_{br}} \left(\frac{m_{bd}}{L_{bd}} \right)^2 \quad [24]$$

$$P_{br} - P_d = \frac{1}{2\rho_{br}} \left(\frac{m_{dd}}{L_{dd}} \right)^2 \quad [25]$$

$$P_{br} - P_b + E_b = \frac{1}{2\rho_b} \left(\frac{m_b}{L_b} \right)^2 \quad \text{with } E_b = -(\rho_b - \rho_{br}) g h_b \quad [26]$$

$$P_{br} - P_d + E_d = \frac{1}{2\rho_d} \left(\frac{m_d}{L_d} \right)^2 \quad \text{with } E_d = -(\rho_d - \rho_{br}) g h_d \quad [27]$$

$$P_b - P_s = \frac{1}{2\rho_{bs}} \left(\frac{m_{bs}}{L_{bs}} \right)^2 \quad [28]$$

$$P_d - P_s = \frac{1}{2\rho_{ds}} \left(\frac{m_{ds}}{L_{ds}} \right)^2 \quad [29]$$

$$P_s - P_{out} + E_s = \frac{1}{2\rho_{cm}} \left(\frac{m_s}{L_s} \right)^2 \quad \text{with } E_s = -(\rho_{cm} - \rho_{out}) g h_s \quad [30]$$

In these equations, h_s , h_b , h_d represent respectively the height of the chimney, the height of the boiler and the height of the DHW heater. The outside pressure at the height of the draft diverters (P_{out}) is taken as the reference pressure, and will be defined as zero.

At this point, the model involves 17 equations and 18 unknowns. The eighteenth unknown is the mean temperature inside the chimney, which is required to compute the mean density in the chimney, ρ_{cm} .

DYNAMIC THERMAL MODELS

Two parameters in the above set of equations, Q_{i_1} and Q_{i_2} , were not precisely defined. These parameters vary with time, depending on the operation of the heating components.

When a heating component (e.g., boiler or DHW heater) is being fired under steady-state conditions, the temperature rise of the gas flowing through that component can be computed from the rate of fuel combustion, and the efficiency with which that energy is being utilized. In other words, because most of the unutilized energy is removed by the air stream, the temperature rise of the air can be related to the mass flowrate of air by the rate of unutilized energy input (i.e., from the stack-gas efficiency of the heater)

When the heater is cycling, the amount of heat input to the air stream depends upon the nature of the cycling, and the dynamic thermal characteristics of the heater component. During a typical cycle, when its thermostat reaches its lower setpoint, the heating system turns on and remains on until the thermostat reaches its upper setpoint. The length of firings, and the length of time between firings depends upon the relationship between the load on the heating system and the capacity of the heater. In the case of a boiler, variations in the thermostat setpoint (e.g., night setback) also affect the cycling of the system. In the particular case of a steam boiler, the phase change also affects the shape of a cycle, as it essentially fixes the maximum temperature of the exhaust gasses.

For given dynamic (i.e., cyclic) conditions, the rate of energy addition to the air stream is controlled by the time constants associated with the heat loss from the various components of the heater. Although there are a large number of time constants corresponding to different components of the system, examination of experimental data from a number of boiler and DHW heaters indicates that the operation can be adequately modeled by two time constants. For a boiler or DHW heater, the two time constants are τ_{fire} , a short-term time constant corresponding to either the mass of the air or the boiler or DHW ductwork, and $\tau_{standby}$, a long term time-constant corresponding to the mass of the water in the system. The rate of energy delivery to the air stream can thus be expressed as:

Steady State:

$$Q_i = (1 - \eta) Q \quad [31]$$

Cycle on:

$$Q_i = (1 - \eta) Q (1 - e^{-\frac{t}{\tau_{fire}}}) \quad [32]$$

Cycle off:

$$Q_i = (1 - \eta) Q e^{-\frac{t}{\tau_{fire}}} \quad [33a]$$

or

$$Q_l = m_b (T_{water} e^{\frac{-t}{\tau_{standby}}} - T_{br}) \quad [33b]$$

During the off cycle, the larger of Equations 33a or 33b are used. The result is that the air leaving the boiler flue is assumed to be at the water temperature whenever the boiler firing is not heating it to a higher temperature. A typical cycle based upon Equations 31-33 is illustrated in Figure 3.

Chimney Model

Due to the typically large vertical rise of the chimney, it is important to have a good estimate of the temperature inside the chimney. The chimney-outside temperature difference is the largest driving force in the system. Also, because of conduction through the chimney walls, the temperature varies along the entire length of the chimney. The problem of predicting the average chimney temperature is complicated further by the presence of thermal mass in masonry chimneys, typically consisting of a square brick duct lined with fireclay brick.

Assumptions

- **Geometric simplifications**

The chimney is well represented by a two dimensional heat transfer model. However, for the purposes of this study, it was further simplified to one-dimensional conduction (plane wall geometry using the average perimeter).

- **Lumped formulation**

The chimney model was developed using lumped parameters at each cross section of the chimney. At each height in the chimney, the heat transfer characteristics were lumped into one thermal capacitance sandwiched between two thermal resistances. Thus, the chimney bricks and liner were assigned a single average time-varying temperature at each height, $T_{brick}(z,t)$. The air flowing through the chimney was also assigned a time-varying average temperature at each height, $T_c(z,t)$. The chimney loses heat to essentially two different temperatures, predominantly the ambient temperature inside the building, but also the outside air temperature. The model presently assumes that the heat loss can be well enough characterized by the mean ambient temperature inside the building (20 °C).

• **Heat transfer coefficients**

The model used to describe the chimney is presented in Figure 4. The effect of conduction along surfaces in contact with the chimney (which act like fins) was ignored. Heat transfer is assumed to occur by free convection on the inside of the chimney, and by free convection and radiation on the outside of the chimney.

The free convection flow regime is determined by the Grashof number, defined as:

$$Gr_l = \frac{g \beta | T_{surface} - T_{air} | l^3}{\nu^2} \quad [34]$$

At Grashof numbers greater than 10^{10} the flow is turbulent, whereas below 10^{10} the flow is laminar.

As the air and surface temperatures driving convection on the inside of the chimney vary with time as the heaters cycle, the flow regime must be examined at a number of temperatures. These temperatures were estimated from field measurements made in a typical chimney, and the fluid-properties ratio, $g\beta/\nu^2$, was computed at a mean film temperature, corresponding to the average of the surface and ambient temperature.¹¹ The length used in Equation 34 is the distance from the bottom to the top of the chimney (12.2 m). Typical results obtained while the boiler was on and off are presented in Table 1.

Table 1: Grashof Numbers Inside the Chimney				
Boiler Condition	$T_{surface}$ [K]	T_{air} [K]	$g\beta/\nu^2$ [1/(K m ³)]	Gr_l [dimensionless]
On	390	453	38×10^6	4.3×10^{12}
Off	315	333	98×10^6	3.2×10^{12}

From the results in Table 1 we deduce that the flow inside the chimney is always turbulent, which allows us to use a simplified relationship for the average heat transfer coefficient based upon an empirically determined constant, K' .¹²

$$\bar{h}_c = K' \frac{(T_{surface} - T_{air})^{\frac{1}{3}}}{\left(\frac{T_{surface} + T_{air}}{2} \right)^{0.41}} \quad [35]$$

The average heat transfer coefficients based upon Equation 35 are presented in Table 2.

Boiler Condition	\bar{h}_c [W/m ² K]
On	5.3
Off	3.9

For the heat transfer by convection along the exterior surface of the chimney, we took the same average brick temperatures as for the previous calculations. However, in this case T_{air} is the ambient temperature of the air surrounding the chimney, which was assumed to be the apartment air temperature, 20°C, and the appropriate length was chosen to be the height of one story (2.4 m). The Grashof numbers and heat transfer coefficients based upon these assumptions are summarized in Table 3. Table 3 also includes the radiative heat transfer coefficients based upon linearization of the radiative heat transfer between the chimney surface and the surrounding surfaces assumed to be at the apartment air temperature (Note: the net radiative heat transport on the inside the chimney is assumed to be zero).

Boiler Condition	$T_{surface}$ [K]	T_{∞} [K]	$g\beta/\nu^2$ [1/(K m ³)]	Gr_1 [dimensionless]	\bar{h}_c [W/m ² K]	\bar{h}_r [W/m ² K]
On	322	293	120 x 10 ⁶	4.8 x 10 ¹⁰	4.7	6.0
Off	301	293	144 x 10 ⁶	1.6 x 10 ¹⁰	3.1	5.2

The Grashof numbers in Table 3 indicate that the flow should be turbulent whether the boiler is on or off. Table 3 also includes radiative heat transfer coefficients based upon the outside surface temperature and the ambient temperature.

Based upon the computed values in Tables 2 and 3, average (independent of temperature) heat transfer coefficients are used in the thermal model of the chimney. The value chosen for the inside of the chimney is 4.6 W/m², whereas the outside heat transfer coefficient chosen is 9.5 W/m². Given the simplified nature of the chimney heat transfer model, we concluded that the errors incurred by using average values for heat transfer coefficients are acceptable.

Network Representation

As was the case for air flow, a network can be used to describe the heat transfer in the chimney. Once again, electrical network symbolism is used: resistors represent the resistance to heat flow by conduction or convection, and capacitors represent thermal mass. From the assumptions described above, the simplified network represented in Figure 5 was derived. In this figure, the two resistors represent the total thermal resistance of the brick and surface layer. The thermal resistance of the brick is split equally on the two sides of the capacitance, which represents the total thermal mass of the bricks and chimney liner.

Chimney Model Derivation

Consider a small element dz of the chimney and apply conservation of energy.

- The network gives us for the bricks:

$$\begin{aligned}
 U_{in} dA_{in} (T_c (z,t) - T_{brick}(z,t)) + U_{out} dA_{out} (T_{amb} - T_{brick}(z,t)) \\
 = \rho_{brick} dV C_{pbrick} \frac{\partial T_{brick}(z,t)}{\partial t}
 \end{aligned}
 \tag{36}$$

where, for a square chimney of inside dimension d and wall thickness e :

$$U_{in} = \frac{1}{\frac{1}{\bar{h}_{in}} + \frac{e}{2k}}
 \tag{37}$$

$$U_{out} = \frac{1}{\frac{1}{\bar{h}_{out}} + \frac{e}{2k}}
 \tag{38}$$

$$dV = e p dz = 4 e (d + e) dz
 \tag{39}$$

$$dA_{in} = 4 d dz
 \tag{40}$$

$$dA_{out} = 4 (d + 2e) dz
 \tag{41}$$

- Equating the rate of energy transfer from the air flowing through the chimney to the heat flux on the inside surface of the chimney yields:

$$m_a C_{p_{air}} (T_c (z+dz, t) - T_c (z, t)) = -U_{in} dA_{in} (T_c (z, t) - T_{brick}(z, t)) \quad [42]$$

By the use of the dimensional constants λ_z [m], λ_t [s], and the thermal conductance ratio, R_U , defined as follows:

$$\lambda_z = \frac{m_a C_{p_{air}}}{4 d U_{in}} \quad [43]$$

$$\lambda_t = \frac{\rho_{brick} e (1 + \frac{e}{d}) C_{p_{brick}}}{U_{in}} \quad [44]$$

$$R_U = \frac{U_{out} dA_{out}}{U_{in} dA_{in}} \quad [45]$$

Equations 36 and 42 can be expressed as:

$$\lambda_z \frac{\partial T_c (z, t)}{\partial z} + T_c (z, t) = T_{brick}(z, t) \quad [46]$$

$$\lambda_t \frac{\partial T_{brick}(z, t)}{\partial t} + (1 + R_U) T_{brick}(z, t) = T_c (z, t) + R_U T_{amb} \quad [47]$$

Chimney Temperature Profile

Equations 46 and 47 are discretized and solved simultaneously by a numerical method. The chimney is divided into equally spaced sections of length Δz along the z axis, with the z -axis origin at the bottom of the chimney. The air temperature T_c and the brick temperature T_{brick} are computed at each of these points. The time space is divided into intervals Δt with time zero taken at the beginning of the simulation. The resulting discretized equations are:

$$T_c (z + \Delta z, t) = T_c (z, t) (1 - \frac{\Delta z}{\lambda_z}) + \frac{\Delta z}{\lambda_z} T_{brick}(z, t) \quad [48]$$

$$T_{brick}(z, t + \Delta t) = \frac{\Delta t}{\lambda_t} T_c (z, t) + R_U \frac{\Delta t}{\lambda_t} T_{amb} + (1 - (1 + R_U) \frac{\Delta t}{\lambda_t}) T_{brick}(z, t) \quad [49]$$

Equation 48 gives at any time t , the chimney air temperature at a point $z + \Delta z$ in terms of the air temperature and the brick temperature at the previous point z . We then need a starting point corresponding to $z=0$, which is the temperature at the bottom of the chimney previously defined as T_{cb} . Equation 49 gives the brick temperature at time $t + \Delta t$ for any point z in the chimney with respect to the previous brick temperature $T_{brick}(z, t)$ and previous chimney air temperature $T_c (z, t)$ at that point.

Thus if we know the temperature profile of the bricks at time zero and the air temperature at the bottom of the chimney at any time t we obtain the flow temperature profile at time t from Equation 48 and the flow temperature profile at time $t+\Delta t$ from Equation 49. These results allow us to deduce the average temperature inside the chimney, T_{cm} , from which we can compute the stack-effect pressure differential.

SOLUTION OF THE SYSTEM OF EQUATIONS

At this stage in the model development we have a system of 18 equations and 18 unknowns which is summarized in Table 4.

Table 4: Summary of Equations and Unknowns		
Unknowns:		
Temperatures	Pressures	Mass flows
T_b	P_{br}	m_b
T_{bs}	P_b	m_{bd}
T_d	P_d	m_{bs}
T_{ds}	P_s	m_d
T_{cb}		m_{dd}
T_{cm}		m_{ds}
		m_s
		m_{br}
Equations: [14-30] [48-49]		

We show in Appendix C that this system of equations can be reduced by straightforward algebra to a system of four equations in four unknown mass flows: m_b , m_d , m_{bd} , m_{dd} . The final reduction of these four equations to one equation in one unknown involves making some assumptions about the physical phenomena inside the chimney.

System Reduction

The four equations for the mass flow rates are expressed in terms of a set of coefficients a_i , all of which are positive and are defined in Appendix C:

$$a_{24}m_d^3 + 2a_1m_d^2 + a_2m_d - a_{25}m_dm_{dd}^2 - a_3m_{dd}^2 - a_4 = 0 \quad [50]$$

$$(a_6 + a_8)m_{bd}^2 + 2a_8m_b m_{bd} + a_9m_{bd} + a_8m_b^2 + a_9m_b - (a_{10} + a_7)m_{dd}^2 - a_{10}m_d^2 - 2a_{10}m_dm_{dd} - a_{11}m_d - a_{11}m_{dd} = 0 \quad [51]$$

$$a_{26}m_b^3 + 2a_{12}m_b^2 + a_{13}m_b - a_{27}m_b m_{bd}^2 - a_{14}m_{bd}^2 - a_{15} = 0 \quad [52]$$

$$a_{23}(m_b + m_d + m_{bd} + m_{dd})^2 + a_{18}m_{bd}^2 + a_{21}(m_b + m_{bd})^2 + a_{22}(m_b + m_{bd}) - a_{20} = 0 \quad [53]$$

From Equations 51 and 53 we can determine m_{bd} and m_{dd} :

$$m_{dd}^2 = \frac{a_{24}m_d^3 + 2a_1m_d^2 + a_2m_d - a_4}{a_3 + a_{25}m_d} \quad [54]$$

$$m_{bd}^2 = \frac{a_{26}m_b^3 + 2a_{12}m_b^2 + a_{13}m_b - a_{15}}{a_{14} + a_{27}m_b} \quad [55]$$

Examination of Equations 54 and 55 shows that they are symmetric equations, Equation 54 representing the flow through the draft diverter of the DHW heater, and Equation 55 the draft diverter flow for the boiler. It is also clear from the manner in which they are expressed that these equations will have two solutions (one negative and one positive). These solutions will either both be real or both be imaginary, depending upon whether or not the right-hand sides of the equations are positive.

To determine whether or not a particular solution can occur, we must step back from the mathematics and examine the physical implications of different situations. Looking first at the flows through the boiler and the DHW heater, m_b and m_d , we should note that it is very unlikely that these flows would be negative. The temperatures inside these components will always be higher than that in the boiler room, and they are isolated from negative flows down the chimney by the draft diverters. On the other hand, negative flows through the draft diverters are quite possible. This will most likely occur at startup of boiler or DHW heater firing, at which time the chimney will not be warm, yet the heaters will be attempting to exhaust a large amount of gas. This situation, in which

gasses pass through the heater and out the draft diverter is known as spillage.

The second situation in which the flows through the draft diverters will be negative occurs when the flow through the chimney is negative, a condition referred to as back-drafting. Backdrafting typically occurs when the chimney is in contact with very cold outdoor temperatures that reduce the chimney temperature below the building air temperature during the off-cycle. Under these conditions, the building will have a stronger stack effect than the actual chimney, thereby inducing flow down the chimney, through the draft diverters into the boiler room and out at the top of the building. This type of negative flow is not likely to occur in the multifamily buildings being studied, as most chimneys in these buildings are not particularly exposed to outdoor temperatures, and most of these chimneys have long time constants which tend to increase the minimum temperature achieved during the off-cycle. For these reasons, the flow model we have derived does not include the stack effect of the building, implying that the only negative flows uncovered by our model will be those due to spillage.

Examining Equations 54 and 55 with these physical constraints in mind, there is only one situation in which the solutions will be imaginary. Namely, because the boiler and DHW heater flows and the a_i coefficients are always positive, the denominators will always be positive, and the numerators will only be negative when m_d is small enough that a_4 dominates, or m_b is small enough that a_{15} dominates. By examining the numerators after solving for the boiler and DHW heater flows, the validity of the solution can be checked directly. Thus, we obtain m_{dd} with respect to m_d and m_{bd} with respect to m_b :

$$m_{dd} = \epsilon_d \sqrt{\frac{a_{24}m_d^3 + 2a_1m_d^2 + a_2m_d - a_4}{a_3 + a_{25}m_d}} \quad [56]$$

$$m_{bd} = \epsilon_b \sqrt{\frac{a_{26}m_b^3 + 2a_{12}m_b^2 + a_{13}m_b - a_{15}}{a_{14} + a_{27}m_b}} \quad [57]$$

The coefficients ϵ_b and ϵ_d are equal to +1 or -1, corresponding to flow into or out of the draft diverter. The present solution technique is to assign these coefficients value +1, and to test the value -1 if no solution to the system of equations is obtained. A successful solution for a coefficient of -1 corresponds to spillage from the heater into the boiler room.

The next step in the solution is to obtain a relationship between m_d and m_b . Rewriting Equation 53 as:

$$a_{23} (m_b + m_d)^2 = a_{20} - a_{18}m_{bd}^2 - a_{21}m_{bd}^2 - a_{22}m_b \quad [58]$$

and solving for m_{ds} yields:

$$m_{ds} = m_d + m_{dd} = \sqrt{\frac{a_{20} - a_{18}m_{bd}^2 - a_{21}m_{bs}^2 - a_{22}m_{bs}}{a_{23}}} - m_{bs} \quad [59]$$

Substituting m_{dd} from Equation 56 into Equation 59, we obtain:

$$\epsilon_d \sqrt{\frac{a_{24}m_d^3 + 2a_1m_d^2 + a_2m_d - a_4}{a_3 + a_{25}m_d}} = M_b(m_b) - m_d \quad [60]$$

where:

$$M_b(m_b) = \sqrt{\frac{a_{20} - a_{18}m_{bd}^2 - a_{21}m_{bs}^2 - a_{22}m_{bs}}{a_{23}}} - m_{bs}$$

Using Equation 57 for m_{bd} and remembering that $m_{bd} + m_b = m_{bs}$, it is clear that M_b is a function of only m_b . If we now square Equation 60 we obtain:

$$\frac{a_{24}m_d^3 + 2a_1m_d^2 + a_2m_d - a_4}{a_3 + a_{25}m_d} = M_b^2 - 2m_dM_b + m_d^2 \quad [61]$$

which can be rearranged into the form:

$$m_d^3 + b_1m_d^2 + b_2m_d + b_3 = 0 \quad [62]$$

in which the b_i coefficients depend only on m_b . However, as the analytical solution for the roots of a cubic equation (Equation 62) depends strongly on the values of the coefficients, and the coefficients are not constant, a general solution cannot be presented here.

Utilizing Equations 56 and 57, Equation 51, like Equation 53, can be rearranged so as to express m_d as a function of m_b . Thus, substituting m_d from Equation 62 and m_{dd} from Equation 56 into Equation 51, we can obtain one equation in one unknown, m_b . Due to the complexity and non-linearity of resulting equation, an analytical solution is impractical. Thus, numerical methods are used to obtain m_b . The numerical method chosen to solve for m_b is the Modified Regula Falsi method.¹³ This method was chosen over Newton's method and the secant's method because of the difficulty in determining the derivative of the equation for m_b , and because Newton's method and the secant's method do not allow for bracketing of the solution.

Algorithm Description

A computer algorithm based upon the above discussion is shown schematically in Figures 6a and 6b. This algorithm is the heart of a computer program for simulating flows in a venting system for two combustion appliances, which is coded in Fortran 77.

The flow of the calculations at any time t is the following:

- Step 0. is to guess a chimney brick temperature profile and chimney mass flowrate at time 0 and to use these values to compute the chimney air temperature profile, and thus the mean chimney air temperature T_{cm} , at time 0 using Equation 48.
- Step 1. is to use the chimney brick temperature profile at time $t-\Delta t$ (the time step, Δt , presently utilized is 60 seconds) to compute the chimney brick temperature profile at time t using Equation 49, and the chimney air temperature profile at time t using Equation 48. The chimney mass flow at time $t-\Delta t$ is used to compute parameter λ_z (given by Equation 43), and Δz is computed from the length of the chimney and number points specified in the input. From the temperature profile inside the chimney we compute T_{cm} and ρ_{cm} .
- Step 2. is to check the time in the boiler and DHW cycling specified for the simulation, in order to specify the coefficients $Q_{lb}(t)$ and $Q_{ld}(t)$.
- Step 3. is to compute all the a_i and b_i coefficients.
- Step 4. is to obtain the roots of the denominators in Equations 56 and 57, establish these as the minimum values for m_b and m_d , and compute initial values for m_d , m_{dd} and m_{bd} with Equations 62, 56 and 57.
- Step 5. is to initiate the Regula Falsi method applied to Equation 51. This is begun by finding a bracket $[a, b]$ for m_b such that the left-hand side of Equation 51, defined as $F(m_b)$, has a different sign at a and b . In other words a and b are chosen such that:

$$F(a) F(b) < 0$$

a is set at the lower limit m_b obtained from Step 4. A fixed increment is added to this value until the sign of $F(m_b)$ changes.

- Step 6. If a bracket for m_b cannot be obtained, the assumed positive signs for either m_{bd} or m_{dd} , or both are assumed to be incorrect, implying spillage. The program then changes the sign of m_{bd} and then m_{dd} , and returns to Step 5. Once the bracket is established the program then iterates until F is within the the user-specified deviation from zero.
- Step 7. is to compute all other unknown values from the solution for m_b obtained in Step 6, and to test that m_s is not significantly from the value used in Step 1. If m_s is significantly different, the program returns to Step 1 and uses the new value of m_s .
- Step 8. is to go back to the time loop and begin Step 1 for time $t+\Delta t$.

Program Input

The input required to run the program includes:

- The physical characteristics of the heating system: leakage areas of each component of the system, height of the boiler stack, DHW stack and chimney, the width of the chimney and of the bricks. The thermal characteristics of the chimney material is presently fixed, but could ultimately be input parameters.
- The outside temperature, the boiler room temperature, the ambient temperature in the house and the cycling characteristics of the boiler and DHW heater.
- The operating characteristics of the heating systems, i.e., the rate of energy input to the boiler and the DHW heater, stack-gas efficiency of the boiler and the DHW heater, and the time constants for heat-up and cool-down.
- Precision limits for iterations.

All of the required input data, excepting the leakage areas, are easy to obtain by measurement:

- Techniques for computing leakage areas are described in Appendix B.

- The time constants for the boiler or the DHW heater can be obtained from the temperature variations inside the boiler or DHW heater during cycling. The short time constant is typically on the order of several minutes, whereas the long time constant typically ranges between five and twenty hours.

COMPARISON WITH MEASURED DATA

Predictions were made with the vent-system flow program based upon data from a six-unit apartment building in Chicago, Illinois. The system in this building corresponds exactly to the multifamily prototype used in our model description. It consists of a single-pipe steam distribution boiler and a tank-type DHW heater venting into a single masonry chimney which rises three stories through the center of the building. The leakage areas of the various components of the system are computed in Appendix B. Physical and thermal characteristics were taken from measurements made in the field; the time constants for the boiler and the DHW were deduced from an analysis of measured flue temperatures. The program input for this building is given in Appendix D.

Some of the results of the simulations performed are presented in Figures 7 and 8. Figure 7 is a plot of the boiler (i.e. boiler-flue), boiler-draft-diverter and boiler-stack flows versus time. It shows that the boiler-draft-diverter flow, the boiler flow, and thus the boiler stack flow increase by about 25% when the boiler turns on. The predicted steady-state flow through the boiler flue of $525 \text{ m}^3/\text{h}$ (room air density) when the boiler is firing corresponds to 100% excess air, which should be compared with 40% excess air ($380 \text{ m}^3/\text{h}$ at room air density) measured by stack-gas analysis of the boiler. Also in Figure 7, the cycling of the DHW heater can be seen in the variations of the boiler-draft-diverter flow. On the other hand, the flow through the boiler flue is basically unaffected by the cycling of the DHW heater.

Figure 8 is a plot of the flows through the DHW vent system components. It shows that like the boiler flue, the the DHW flue flow does not depend on the operation of the other combustion appliance. The predicted flow through the DHW flue ($140 \text{ m}^3/\text{h}$ at room air density) during DHW firing corresponds to 170% excess air, which seems excessively high, and probably implies a poor estimate of the flow resistance of the DHW heater. Figure 8 also shows that the change in flow through the DHW draft diverter during boiler operation is more dramatic than the change in the boiler-draft-diverter flow during DHW operation. This is not surprising, as boiler operation has a larger effect on chimney temperature, and therefore on the stack pressure produced.

The predictions of vent system flows were compared with some overnight flow measurements made in the field. These results are presented in Table 5.

Table 5: Measured and Predicted Flowrates in Chicago Apartment Building.			
System Operation	Location	Measured Flow [m ³ /h, 24 °C]	Predicted Flow [m ³ /h, 24 °C]
Boiler off, DHW off	Chimney	1100	1100
	Boiler Flue	350-500	430
	DHW Stack	200	220
Boiler off, DHW on	Chimney	1150	1200
	Boiler Flue	350-500	410
	DHW Stack	220	250

Table 5 indicates that the predicted flows are close to the measured values, indicating that the model can provide reasonable estimates of flows through two-appliance venting systems. However, although the comparison in Table 5 is encouraging, a more comprehensive validation of the model is needed. Such a validation should include a more detailed analysis of the measured data and predictions for several different systems, and should include simultaneous measurements of temperatures and flows under different weather and operating conditions.

FUTURE WORK

The work described in this report has provided us with a tool that can be used to evaluate the performance of venting systems for multiple combustion appliances. The model developed is capable of predicting the energy savings that can be expected from vent dampers, including the effects of damper tightness and pilot cutouts on energy savings and spillage. The model can also be used to examine the effectiveness of installing DHW vent dampers in addition to boiler vent dampers.

The comparison of model flow predictions with measured results indicates that the program developed can provide reasonable estimates of the flow through a two-appliance venting system. However, due to the limited nature of the measured data and the analysis performed, a more complete validation of the model should be performed.

One aspect of the model development that was not tested is the simplified thermal model presently being used for the chimney. As the objective of the chimney model is to obtain an estimate of the mean chimney gas temperature as a function of time, and the mass flowrate up the chimney is sensitive to this temperature, this model should be compared with an exact model of the heat transfer in the chimney, examining differences in mass flowrates and energy flowrates. A careful examination of the chimney model may

also be warranted by the interest in testing the savings potential of metal chimney liners, which should have time constants much shorter than masonry units. These short time constants should reduce the driving force for off-cycle chimney losses.

Our vent damper model is presently limited to electronic dampers, which open and close essentially instantaneously. A number of boilers are presently being fitted with thermally activated dampers, which are inherently slower to react to heating appliances being turned on or off. Depending upon the frequency of cycling, this type of operation could be significantly different from that of instantaneous-response dampers. The magnitude of this effect should be examined, and the program potentially modified to model leakage areas which vary with temperature.

Finally, once we are satisfied with the validity of the model, the model should be used to examine the energy savings that can be expected over an entire heating system for various types of vent damper retrofits. Multiple simulations could ultimately be used to develop simplified evaluation tools to be incorporated into multifamily building energy audits.

ACKNOWLEDGMENT

The authors would like to thank John Katrakis and his staff at the Center for Neighborhood Technology for their invaluable assistance in this study. The authors would also like to thank Darryl Dickerhoff for his patient examination of all the equations in this report.

REFERENCES

1. R.C. Diamond, et. al., "Building Energy Retrofit Research- Multifamily sector, Multiyear plan FY 1986 - FY 1991", August 1985, Lawrence Berkeley Laboratory Report LBL-20165.
2. M.P. Modera, J.T. Brunsell, R.C. Diamond, "Improving diagnostics and energy analysis for multifamily buildings: a case study", Proceedings of Thermal Performance of the Exterior Envelopes of Buildings Conference III, ASHRAE/DOE/BTECC, Clearwater FL, December 1985, Lawrence Berkeley Laboratory Report LBL-20247.
3. M. Hewett, M. Koehler, "Tests of vent dampers in multifamily buildings: preliminary results", October 1985, Minneapolis Energy Office, Room 330, City Hall, Minneapolis, MN.
4. M. Hewett, et. al., "Measured energy savings from vent dampers in low-rise apartment buildings", April 1985, Minneapolis Energy Office, Room 330, City Hall, Minneapolis, MN.
5. M. P. Modera, R. C. Sonderegger, "Determination of in-situ performance of fireplaces", August 1980, Lawrence Berkeley Laboratory Report LBL-10701.
6. U. Bonne, J. E. Janssen, L. W. Nelson and R. H. Torborg, "Control of overall thermal efficiency of combustion heating systems", 16th Symposium on Combustion, MIT, Cambridge, Massachusetts, 1976.
7. M. C. Swinton, et. al., "The thermal and flow performance of furnace flues in houses: summary report" Scanada Consultants Limited, Ottawa, Ontario Canada, March 1985.
8. H. E. Feustel, et. al., "Temperature- and wind-induced air flow patterns in a staircase - computer modeling and experimental verification", Energy and Buildings, 8 (1985), Lawrence Berkeley Laboratory Report LBL-14589, August 1985.
9. W.M. Kays and M.E. Crawford, *Convective heat and mass transfer*, MacGraw-Hill series in Mechanical Engineering, 1980.
10. ASHRAE Handbook of Fundamentals, Chapter 33, 1981, American Society of Heating, Refrigerating and Air-Conditioning Engineers, Atlanta, GA.

11. F. Krieth, *Principles of Heat Transfer*, 3rd Edition, Intext Press, 1973, New York, New York.
12. M. P. Modera, "Monitoring the heat output of a wood-burning stove", *Heat Transfer Engineering*, Volume 7, Nos. 1-2, 1986, pages 25-35.
13. F. S. Acton, *Numerical methods that work*, Harper and Row, New York, 1970.

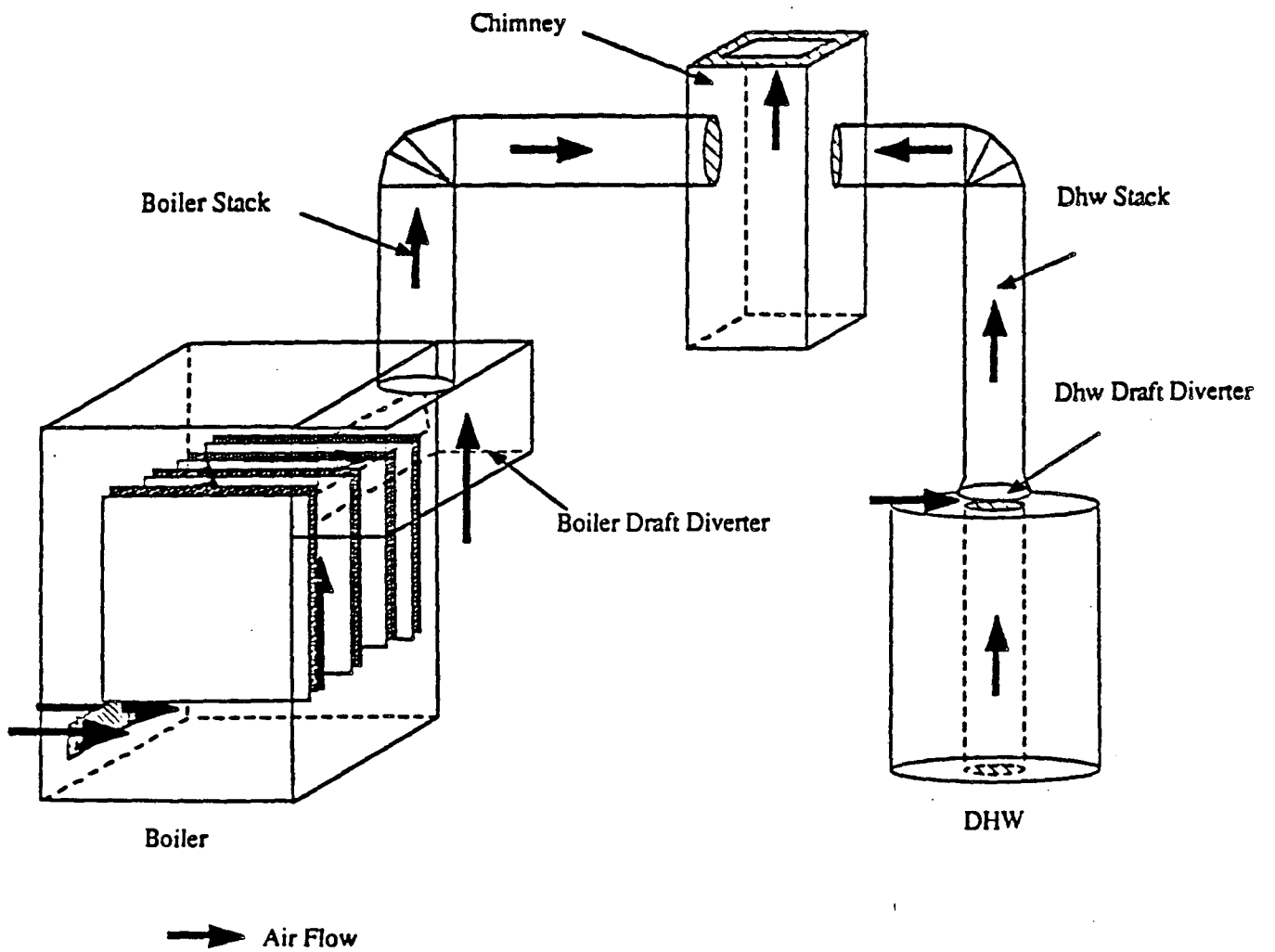


Figure 1: Venting system flow path.

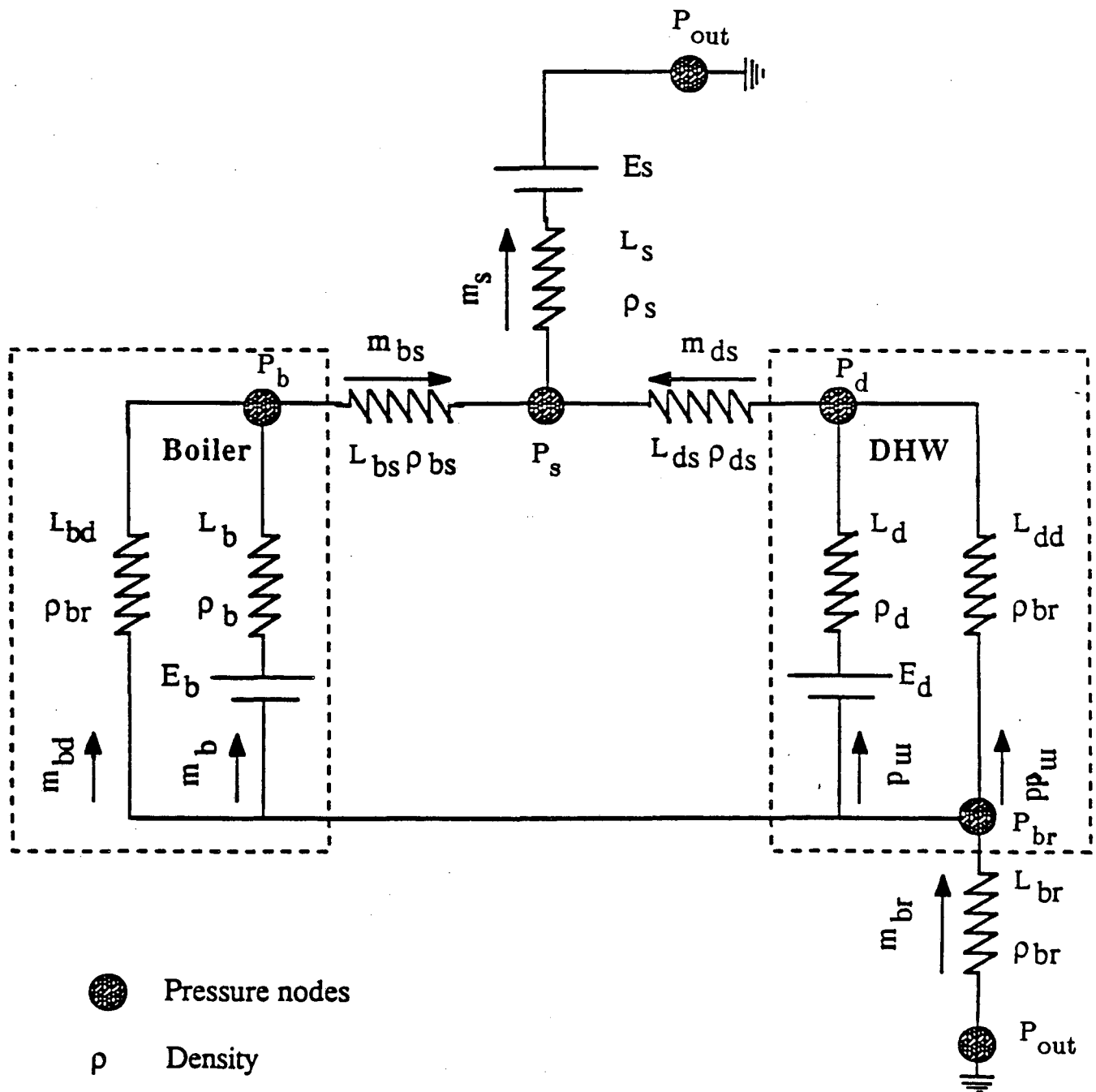


Figure 2: Network representation of venting system.

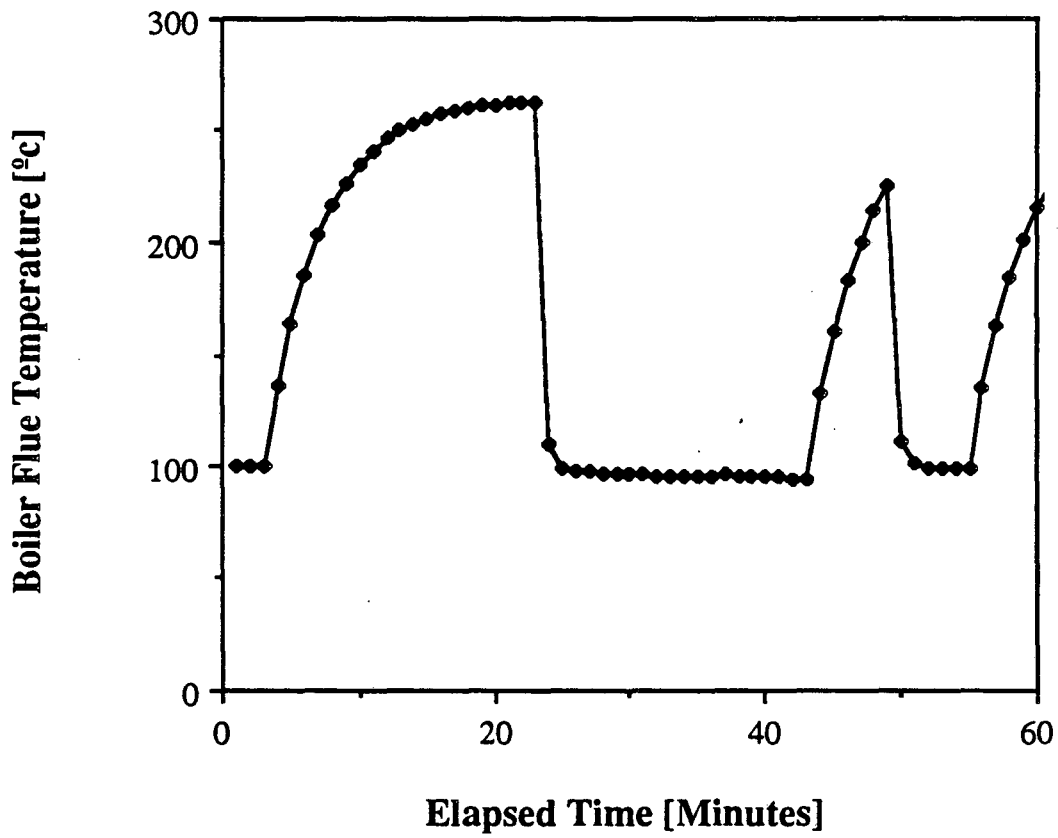


Figure 3: Variation of boiler flue temperature during boiler cycling.

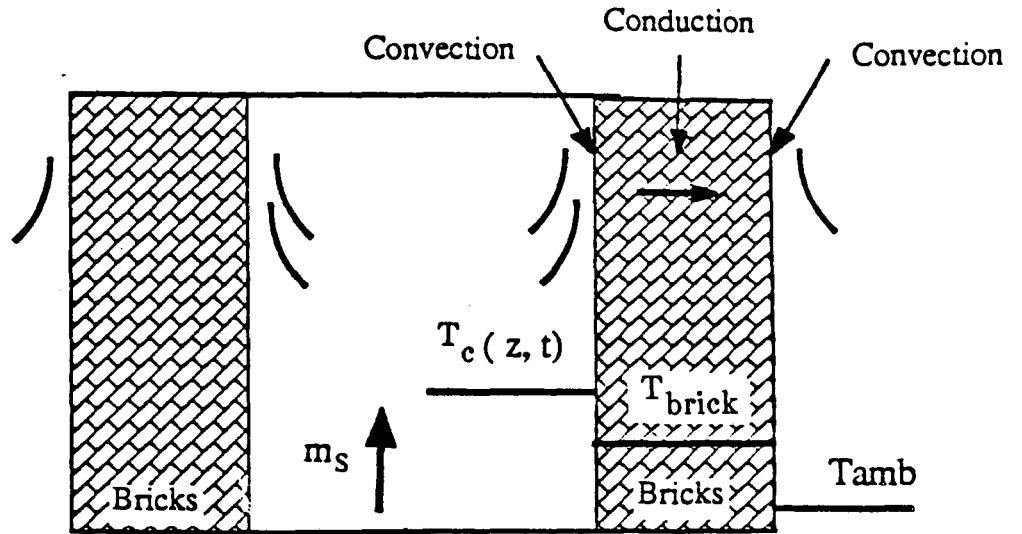


Figure 4: Schematic description of heat transfer through the chimney.

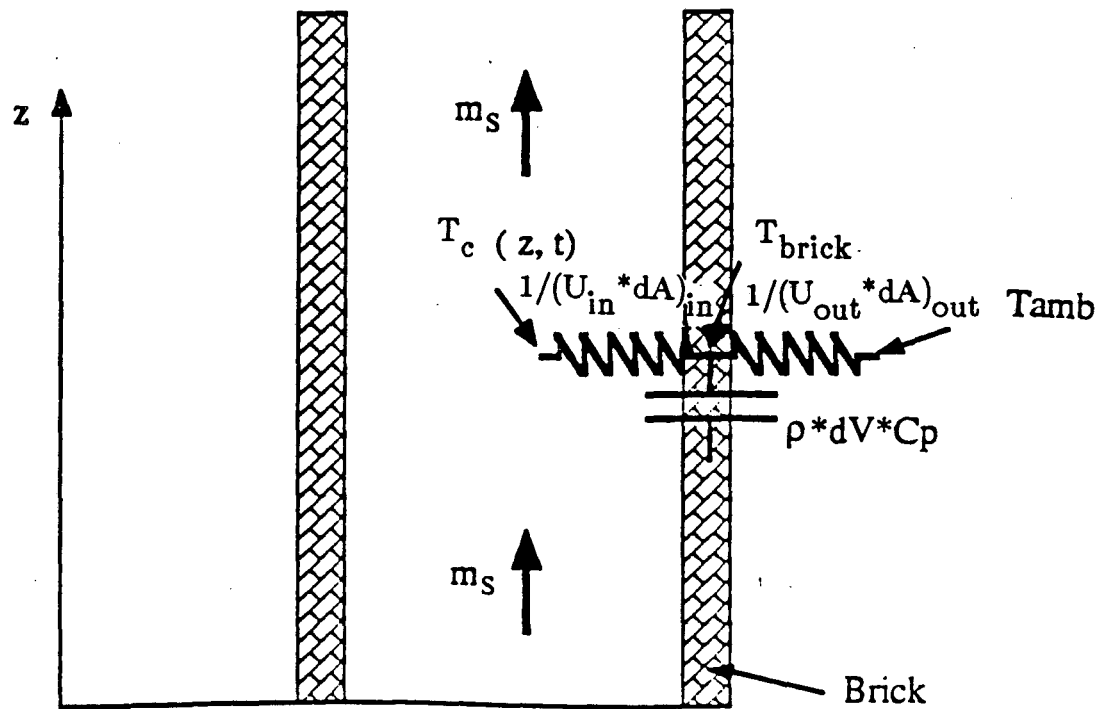


Figure 5: Network model of heat transfer through the chimney.

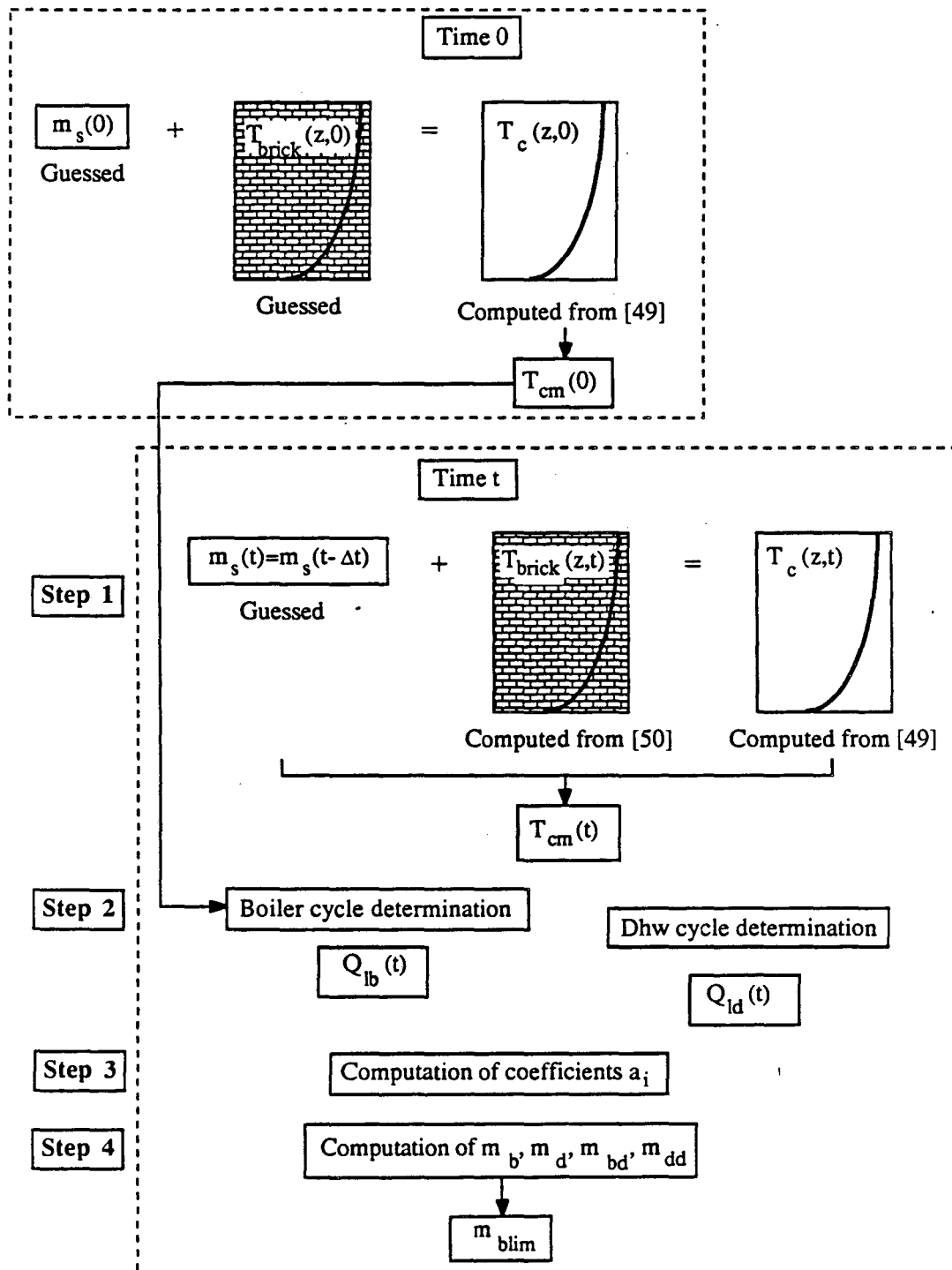


Figure 6a: Flow diagram for simulation program.

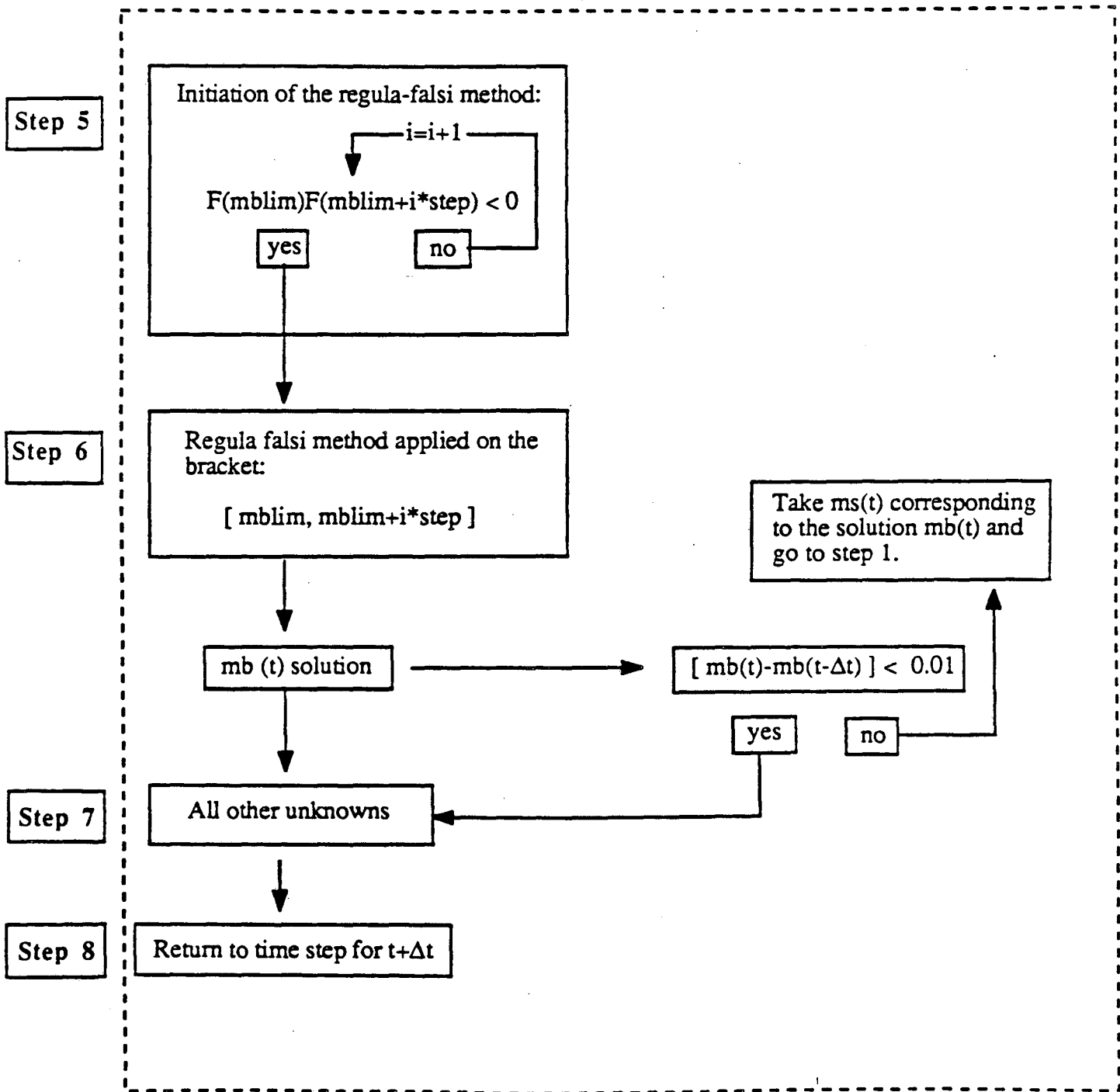


Figure 6b: Flow diagram for simulation program (con't).

Boiler Flows

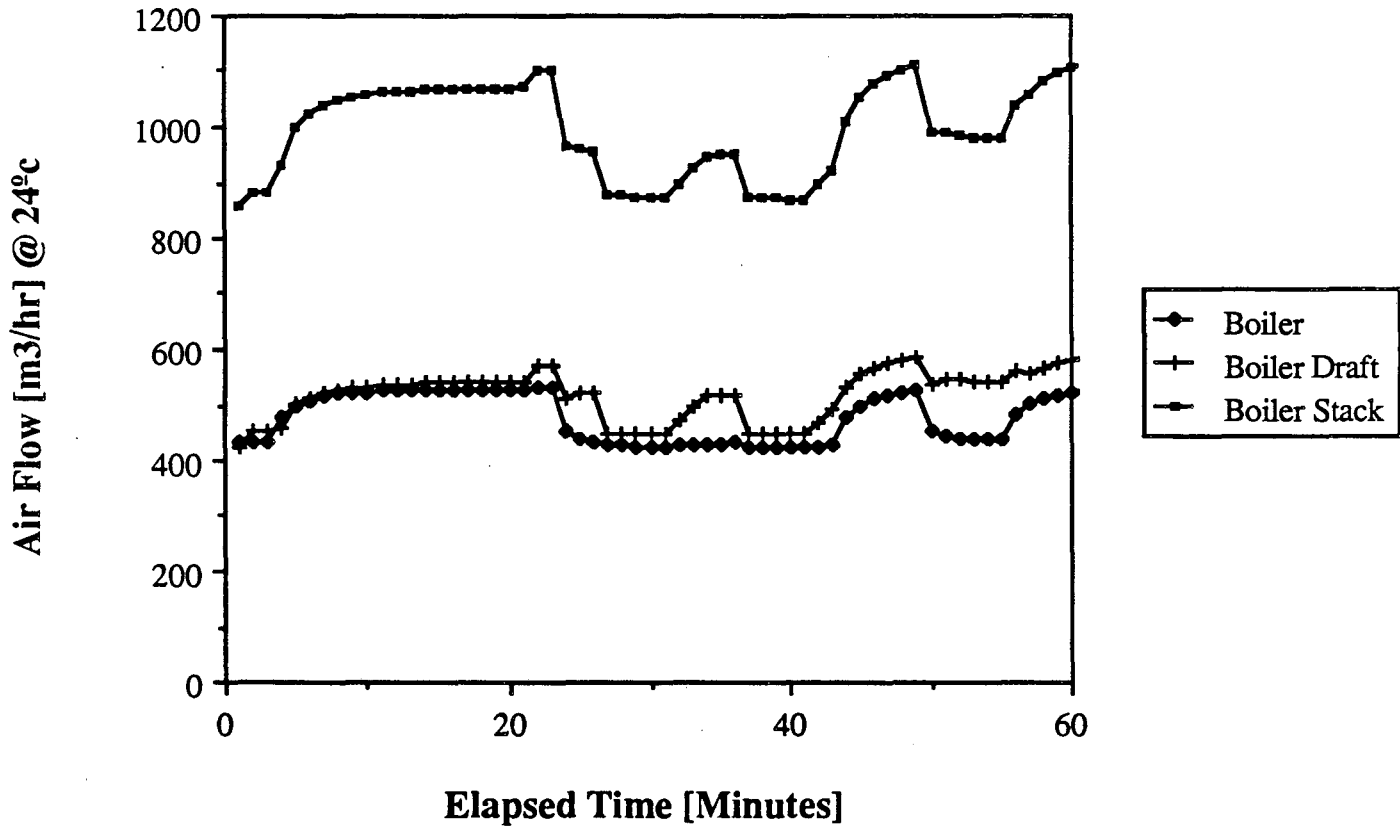


Figure 7: Simulated air flows through boiler vent system. All flows are at room temperature density ($T_{out} = 10^{\circ}C$).

Dhw Flows

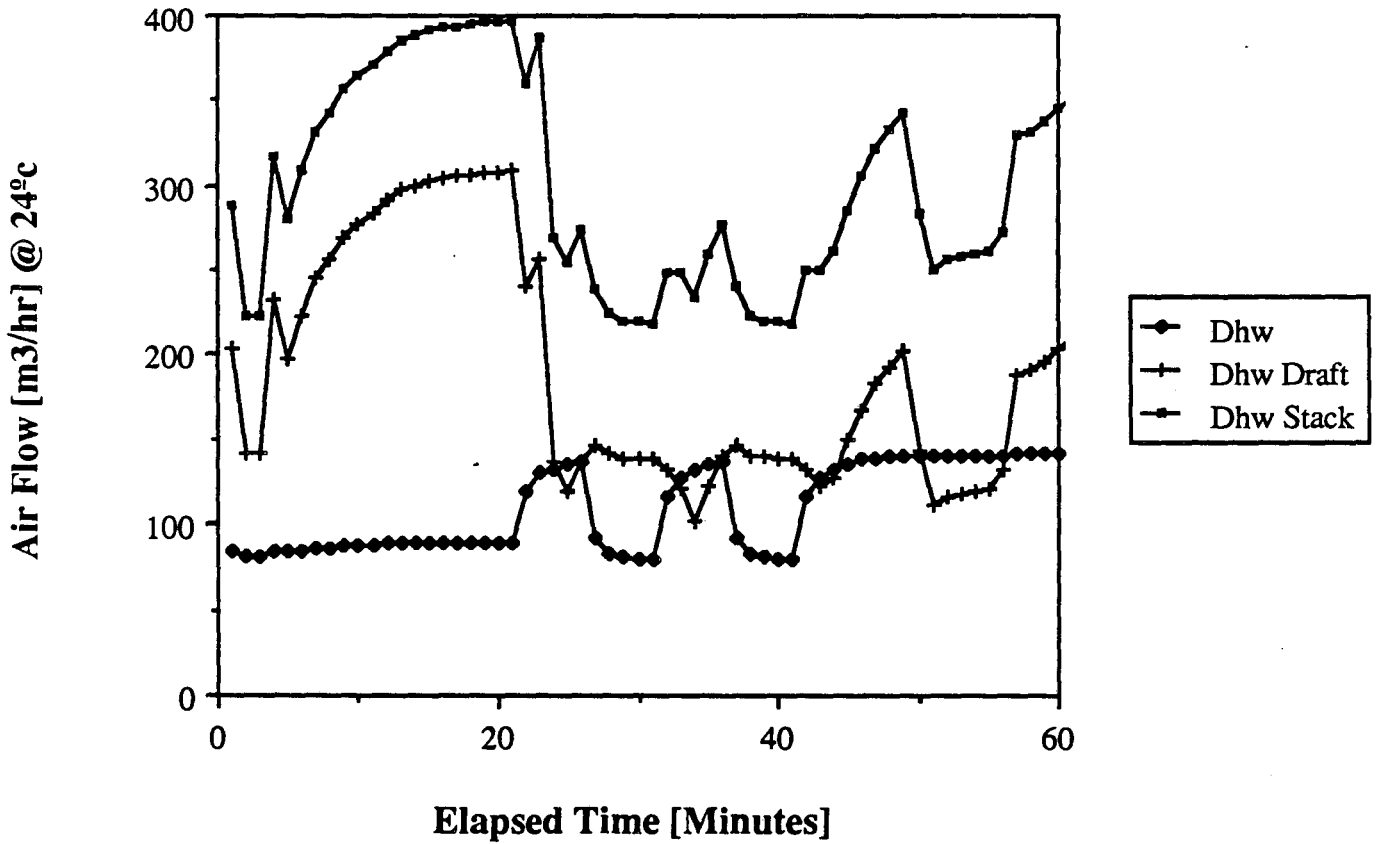


Figure 8: Simulated flows through DHW vent system. All flows are at room temperature density ($T_{out}=10^{\circ}C$).

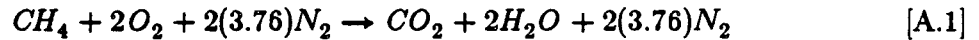
APPENDIX A

EFFECTS OF GAS COMPOSITION VARIATION

Inside the boiler or the DHW heater, combustion changes the composition of the gasses flowing through the system. At the combustion-appliance entrance, the flow made up solely of air, whose composition is approximated by:

$$\begin{array}{l} 21\% \text{ O}_2 \\ 79\% \text{ N}_2 \end{array}$$

The fuel, natural gas, enters separately through a pipe to the burner. Natural gas is basically methane (CH_4), which reacts with air according to the relation:



As air is made up of N_2 and O_2 , the volume of dry air required to supply a given volume of oxygen is 4.76 times the volume of oxygen required. However, because combustion rarely occurs at stoichiometric conditions, the possibility of additional air flow not participating in the combustion process must be accounted for. The traditional parameter used to describe this effect is the percentage excess air:

$$\% \text{ Excess air} = 100 \left(\frac{Q_{\text{air}}}{9.52 Q_{\text{CH}_4}} - 1 \right) \quad [\text{A.2}]$$

where:

- Q_{air} is the volume rate of air flow into the boiler, and
- Q_{CH_4} is the volume rate of natural gas flow into the boiler.

Thus, the choice of an appropriate density in the flow simulation for the flow leaving the heaters during firing depends upon the relative densities of the constituent gasses, and on the relative fractions of these gasses (which in turn depends upon the % excess air). Using Equation A.1, and including the possibility of excess air in the exhaust gasses, the average density of the gasses leaving the combustion zone can be written as:

$$\rho_{\text{exhaust}} = \frac{\rho_{\text{air}} Q_{\text{air}} + \rho_{\text{N}_2} Q_{\text{N}_2} + \rho_{\text{CO}_2} Q_{\text{CO}_2} + \rho_{\text{H}_2\text{O}} Q_{\text{H}_2\text{O}}}{Q_{\text{exhaust}}} \quad [\text{A.3}]$$

Because we are dealing with gasses, their densities simply depend on their molecular weights, which are summarized for the gasses involved in Table A.1.

Table A.1 Molecular Weights of Combustion Gasses						
Gas	Air	O ₂	N ₂	CH ₄	CO ₂	H ₂ O
Mol Weight	29	32	28	16	44	18

Thus, the density the constituent gasses can be expressed as the ratio of their molecular weight to the molecular weight of air times the density of air. Utilizing this relationship and the definition of % excess air in Equation A.3 yields:

$$\rho_{exhaust} = \rho_{air} \left(1 - \frac{0.045}{\frac{\%excessair}{100} + 1.1} \right) \quad [A.4]$$

The error induced by using the density of air rather than the exact density of the exhaust gasses can be determined directly from Equation A.4. Some example values for this error for different values of % excess air are presented in Table A.2.

Table A.2 Density Errors Incurred by Using Air Rather Than Exact Composition of Exhaust Gasses During Combustion	
Excess Air [%]	Error [%]
0	4.3
20	3.6
50	2.9
100	2.2
200	1.0

The results in Table A.2 show that the error induced by using air density for the density of the exhaust gasses is at most 4.3%. The other error that could be induced by using air rather than the correct gas composition is that due to an error in specific heat. A similar analysis shows that this error is always less than 16%, and in the opposite direction, implying that the maximum error is 12%, and occurs at 0% excess air.

APPENDIX B

LEAKAGE AREA COMPUTATION TECHNIQUES

This appendix describes techniques for computing the leakage areas used as input to the vent-flow program. Most calculations are based on the ASHRAE Handbook of Fundamentals (Reference 10) in which fitting loss coefficients (K) are tabulated. To choose the appropriate loss coefficient for a given vent-system component, certain geometric simplifications are often necessary. These simplifications, as well as an example calculation for a multi-family building venting system, are described in this Appendix.

Flow Resistance Formalism

As described in the main text, all pressure losses in the venting system are assumed to be proportional to the square of the mass (or volume) flowrate, including dynamic pressure losses and turbulent frictional losses. Under such conditions the resistance to flow can be expressed in a number of different formalisms. As input to the flow prediction program, leakage area, which can be thought of as effective flow area, is the chosen formalism:

$$L = C_l A = \frac{A}{\sqrt{K}} \quad [10]$$

where:

C_l is the effective area fraction [dimensionless] used to compute the flowrate according to the relation:

K is the fitting loss coefficient [dimensionless] tabulated in the ASHRAE Handbook of Fundamentals as C_o .

$$\Delta P = \frac{m^2}{2 \rho C_l^2 A^2} = \frac{m^2}{2 \rho L^2} = K \frac{m^2}{2 \rho A^2} \quad [B.1]$$

Combining Resistances in Series or in Parallel

To compute the leakage area of a venting system component consisting of multiple subcomponents with known leakage areas involves application of the law of continuity (mass conservation), in which leakage areas are treated as inverse flow resistances. However, for the turbulent flows encountered in vent systems, mass flow is not linearly related to pressure difference, implying that the simplified relationships developed for adding

linear resistances cannot be utilized. Thus, a new set of simplified relationships must be derived for turbulent flow conditions.

- Considering N resistances in **series**, the relation between the pressure difference and the mass flow in section i of the flow path is:

$$P_{i-1} - P_i = \frac{K_i}{A_i^2} \frac{m_i^2}{2\rho} \quad [\text{B.2}]$$

where:

K_i is the fitting loss coefficient obtained from the ASHRAE handbook [dimensionless].

As m_i is constant in a series connection of flow resistances, the total pressure difference is the sum of the individual pressure differences:

$$P_0 - P_N = \sum_i \frac{K_i}{A_i^2} \frac{m^2}{2\rho} = \frac{K}{A_n^2} \frac{m^2}{2\rho} \quad [\text{B.3}]$$

Thus, the equivalent fitting loss coefficient K_{equ} is:

$$K_{equ} = A_n^2 \sum_i \frac{K_i}{A_i^2} \quad [\text{B.4}]$$

the equivalent leakage area coefficient $C_{l,eq}$ is:

$$C_{l,eq} = \frac{1}{\sqrt{A_n^2 \sum_i \frac{1}{C_{li}^2 A_i^2}}} \quad [\text{B.5}]$$

and the equivalent leakage area L_{equ} is:

$$L_{equ} = \frac{1}{\sqrt{\sum \frac{1}{L_i^2}}} \quad [\text{B.6}]$$

- Considering N resistances in **parallel**, the pressure drop across all resistances is now the same, but the mass flow m_i is different for each resistance. The total flow through the component will be the sum of the individual mass flows m_i :

$$m = \sum_i m_i = \sum_i \left(\frac{A_i}{\sqrt{K_i}} \right) \sqrt{2\rho \Delta P} \quad [\text{B.7}]$$

Thus, in a parallel configuration, the equivalent fitting loss coefficient K_{equ} of the net-

work is given by the relation:

$$K_{eqv} = \left(\frac{\sum_i A_i}{\sum_i \frac{A_i}{\sqrt{K_i}}} \right)^2 \quad [B.8]$$

the equivalent leakage area coefficient C_l is:

$$C_{l,eqv} = \frac{1}{\sum_i A_i} [\sum_i A_i C_{l,i}] \quad [B.9]$$

and the equivalent leakage area L_{eqv} is:

$$L_{eqv} = \sum L_i \quad [B.10]$$

Leakage Area Coefficient for Frictional Losses

To add flow resistance due to frictional losses to resistances resulting from dynamic losses, both losses must be expressed in the same formalism. Thus, the leakage area coefficient for frictional losses is:

$$C_l = \sqrt{\frac{D}{f l}} \quad [11]$$

D in Equation 11 is the hydraulic diameter, defined as:

$$D = 4 \frac{\text{Cross sectional area}}{\text{Perimeter}}$$

As an example, for a square chimney with inside dimension d, the hydraulic diameter is:

$$D = 4 \left(\frac{d^2}{4 d} \right) = d$$

f in Equation 11 is the friction factor. It depends on the Reynolds number and on the relative roughness coefficient, defined as the ratio of the roughness height ϵ to the hydraulic diameter D. Values for the friction factor can be obtained from the ASHRAE Handbook of Fundamentals. For the example system in the main text, f was computed from the values in Table B.1.

Roughness height ϵ [m]	0.0015
Diameter D [m]	0.38
Relative roughness ϵ/D	0.004
Reynolds number Re	44000
Friction factor f	0.031

The roughness height in Table B.1 was taken from the ASHRAE Handbook of Fundamentals for clay pipe. The Reynolds number of 44000 was chosen based on a flowrate of 1000 standard m³/hr and temperature of 60°C measured in the chimney during the off-cycle. For this Reynolds number and relative roughness $f=0.031$. Finally, $l (=h_s)$ is the length of the chimney in meters.

Due to the complex structure of venting systems, it would be awkward and lengthy to compute the flow resistance exactly for all components. Thus, one simplification that can be made is to neglect friction losses relative to dynamic losses whenever possible.

Considering a pipe of internal diameter D and length l :

The dynamic loss coefficients corresponding to the entrance and to the exit of the pipe (from ASHRAE fitting loss coefficients) are given by:

- Entrance of the pipe:

$$C_{l_{\text{entrance}}} = \frac{1}{\sqrt{0.5}} = 1.414 \quad [\text{B.11}]$$

- Exit of the pipe:

$$C_{l_{\text{exit}}} = \frac{1}{\sqrt{1}} = 1 \quad [\text{B.12}]$$

- Using our example duct characteristics to determine the frictional loss coefficient we obtain:

$$C_{l_{\text{friction}}} = \sqrt{\frac{D}{0.031 l}} \quad [\text{B.13}]$$

Thus, to compare frictional and dynamic losses we compare the flow resistances associated with these losses, where:

$$R = \frac{1}{2\rho (C_1 A)^2} \quad [\text{B.14}]$$

As the cross sectional area A and the density ρ are the same for all three losses, we will just compare the coefficients $1/C_1^2$. Thus, the total dynamic resistance is $1.5(1/2\rho A^2)$ and the frictional resistance is $(0.031 l/D)(1/2\rho A^2)$. The error caused by neglecting the frictional losses in the total loss evaluation is:

$$\frac{R_{\text{approximate}}}{R_{\text{actual}}} = \frac{1.5}{1.5 + 0.031 \frac{l}{D}} \quad [\text{B.15}]$$

If we want to limit the error to 10%, we should have:

$$0.9 \leq \frac{R_{\text{approximate}}}{R_{\text{actual}}} \quad [\text{B.16}]$$

which gives us the following condition for the ratio l/D :

$$\frac{l}{D} \leq 5.4 \quad [\text{B.17}]$$

For a galvanized duct, due to the reduced roughness height, the condition for l/D becomes:

$$\frac{l}{D} \leq 7.3 \quad [\text{B.18}]$$

Thus, for galvanized sheet metal ducts at high Reynolds numbers, whenever the length of the pipe is less than 7 times the internal diameter of the pipe we can neglect frictional losses with less than a 10% error.

Multifamily Boiler-DHW Example

A schematic representation of the flow path through a typical multifamily boiler is presented in Figure B.1. The flow resistance of this system is obtained from the fitting loss coefficients in the 1981 ASHRAE Handbook of Fundamentals (which will be referred to as the ASHRAE Handbook).

Boiler

The flow path through the boiler was modeled as six resistances in series:

- A rectangular entrance partially obstructed by 5 circular cylinders.

- A diffuser-elbow section.
- A heat exchanger modeled as five thin parallel rectangular ducts.
- An elbow section.
- A contraction.
- A cross-flow exit.

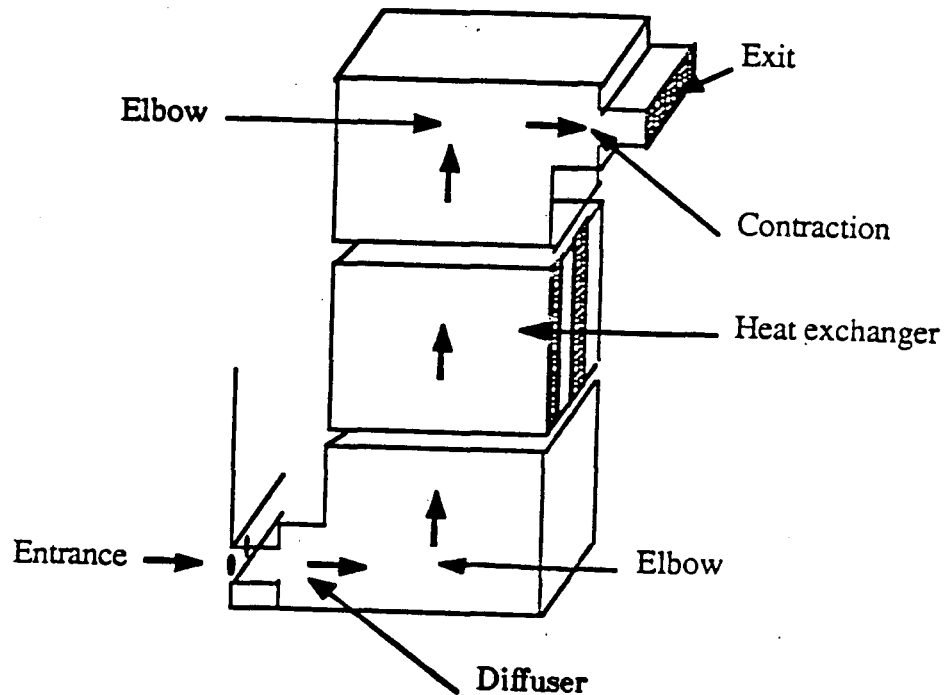


Figure B.1

1. The partially-blocked rectangular entrance was treated as a simple rectangular entrance with the same open area as that of the rectangular entrance minus the area blocked by the cylinders (see Figure B.2). The fitting loss coefficient is taken from the ASHRAE Handbook, Table B-1, Section 1.1, page 33.28, with $L=0$ and $t=0$.

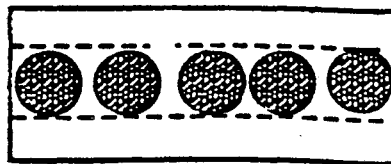


Figure B.2

The resistance of the entrance can then be described by:

$$K_{\text{entrance}} = 0.5 \quad C_{l_{\text{entrance}}} = 1.4 \quad A_{\text{entrance}} = 0.10 \text{ m}^2$$

2. For the diffuser-elbow, the ASHRAE Handbook provides the fitting loss coefficients corresponding to elbows in Table B-3, Section 3.10, page 33.32. The parameters chosen for use in the ASHRAE table are summarized in Table B.2.

H0	0.61 m	W0	0.23 m	H0/W0=2.3
H1	0.81 m	W1	1.0 m	W1/W0=4.4

These values were out of the range given in the ASHRAE table. The results in the ASHRAE table were plotted and an extrapolation was made, resulting in a fitting loss coefficient of 0.6, which when multiplied by $K_{Re}=1.4$ (corresponding to a Reynolds number of 10000) yielded a fitting loss coefficient of:

$$K_{\text{elbow}} = 0.84 \quad C_{l_{\text{elbow}}} = 1.09 \quad A_{\text{elbow}} = 0.10 \text{ m}^2$$

3. The heat exchanger is modeled as five thin parallel rectangular ducts represented as five identical resistances in parallel, each resistance corresponding to one of the five rectangular ducts (see Figure B.3).

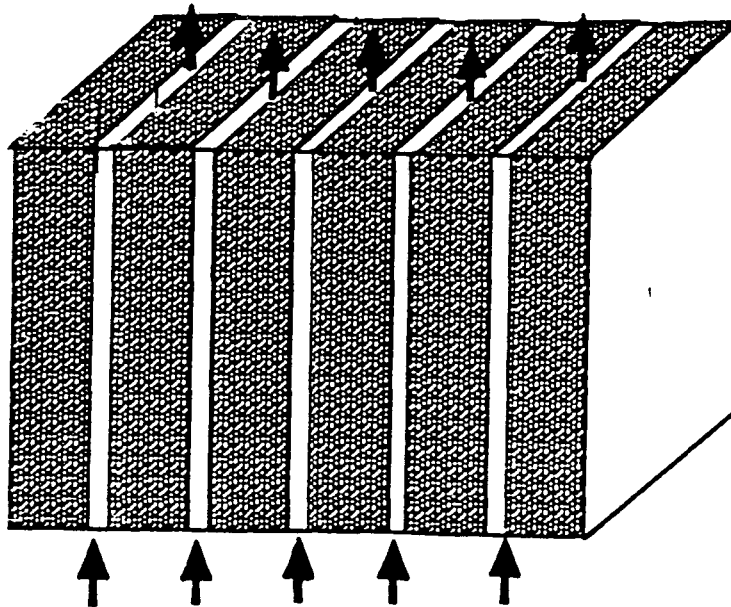


Figure B.3

As all the ducts are the same, calculations are made for one duct. Pressure losses in this duct include dynamic losses at the entrance, frictional losses to the walls and flow divergence losses at the transition from the ducts to the elbow. The dynamic losses at the entrance correspond to a contraction, and ASHRAE Handbook Table B-5, Section 5.1, page 33.35 is used. With an area ratio $A_1/A_0 = 0.81/0.125 = 6.5$, the entrance losses referenced to the heat exchanger area are:

$$K_{\text{entrance}} = 0.42 \quad C_{l_{\text{entrance}}} = 1.54 \quad A_{\text{heat exchanger}} = 0.125 \text{ m}^2$$

For the frictional losses, the hydraulic diameter was taken as:

$$D = 4 \frac{A}{P}$$

which gives us:

$$D = 4 \frac{(1.0 \cdot 0.025)}{(2(1.0 + 0.025))} = 0.049 \text{ m}$$

The friction factor was obtained with Equation 11, using a duct length of 1.12 m and a Reynolds number of approximately 1000 (The Reynolds number will be lower when the boiler is firing, as the mass flowrate does not change significantly, but the temperature increases). This Reynolds number is in the laminar regime, which implies that $f=64/Re=0.07$, and:

$$K_{\text{friction}} = 0.07 \frac{1.12}{0.049} = 1.6$$

The diffuser loss coefficient is taken from the ASHRAE Handbook, Table B-4, Section 4.3, page 33.33. It corresponds to a 180 degree diffuser for which $A_1/A_0=6.5$. The value obtained by extrapolation for the fitting loss coefficient is 0.85, and the corresponding leakage area coefficient is 1.08.

Using Equations B.4 to combine resistances in series, the fitting loss coefficient corresponding to one duct of the heat exchanger is obtained:

$$K = 0.42 + 1.6 + 0.85 = 2.9$$

Using Equation B.7 to combine the five ducts, the overall fitting loss coefficient, leakage area coefficient and flow area of the heat exchanger are:

$$K_{\text{heat exchanger}} = 2.9 \quad C_{l_{\text{heat exchanger}}} = 0.59 \quad A_{\text{heat exchanger}} = 0.125 \text{ m}^2$$

4. The elbow section losses are computed from the ASHRAE Handbook, Table B-3, Section 3.10, page 33.32, using the parameter values summarized in Table B.3.

H0	0.81 m	W0	1.0 m	H0/W0=0.81
H1	0.81 m	W1	0.30 m	W1/W0=0.30

The following results were estimated by extrapolation:

$$K_{\text{elbow}} = 3.0 \quad C_{l_{\text{elbow}}} = 0.58 \quad A_{\text{elbow}} = 0.81 \text{ m}^2$$

5. The exit contraction losses are determined from Table B-5, Section 5.1, page 33.35 of the ASHRAE Handbook. By specifying $\theta=180$ degrees and $A1/A0=0.31/0.12=2.6$, the following results were obtained:

$$K_{\text{contraction}} = 0.30 \quad C_{l_{\text{contraction}}} = 1.83 \quad A_{\text{contraction}} = 0.126 \text{ m}^2$$

6. The exit cross-flow fitting loss coefficient is taken from the ASHRAE Handbook, Table B-6, Section 6.6, page 33.37. The geometrical description of the cross flow is given in Figure B.4.

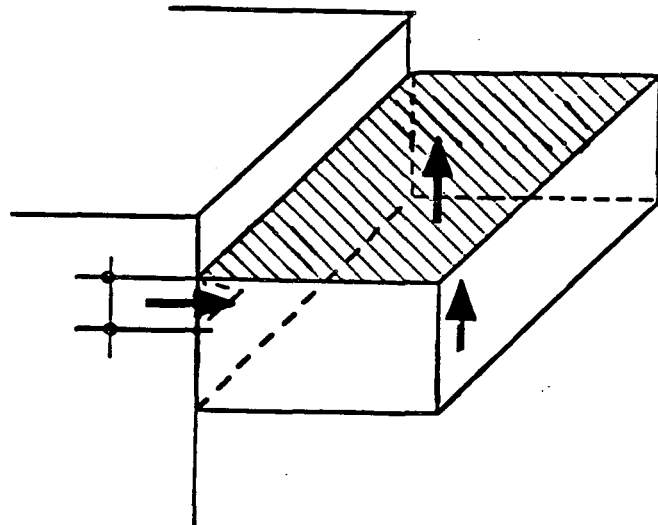


Figure B.4

To compute the cross-flow losses, measurements made in the field under a typical boiler off-cycle period were used:

$$A_b/A_s=0.44$$

$$V_c=0.8 \text{ m/s} \leq 6 \text{ m/s}$$

$$Q_b = 300 \text{ m}^3/\text{h}$$

$$Q_s = 530 \text{ m}^3/\text{h}$$

$$Q_c = 830 \text{ m}^3$$

So Q_b/Q_c is 0.36, which yields a fitting loss coefficient corresponding to the cross flow exit of 0.19. To reference this pressure to the flow through the boiler exit it must be multiplied by the square of the velocity ratio between the stack and the exit 1.28^2 , which yields:

$$K_{\text{cross-flow exit}} = 0.31 \quad C_{l_{\text{cross-flow exit}}} = 1.8 \quad A_{\text{cross-flow exit}} = 0.13 \text{ m}^2$$

The pressure losses for each subcomponent of the boiler are summarized in Table B.4.

Subcomponents	C_l	Area (m ²)	L (m ²)	1/L ²
Entrance	1.4	0.10	0.14	51 (15%)
Diffuser-elbow	1.1	0.10	0.11	83 (24%)
Heat exchanger	0.59	0.13	0.077	169 (49%)
Elbow	0.58	0.81	0.47	5 (1%)
Exit contraction	1.8	0.13	0.23	19 (5%)
Exit cross flow	1.8	0.13	0.23	19 (5%)
Total (effective)			0.054	346 (100%)

Boiler Draft Diverter

The boiler draft diverter is a rectangular box connected to the boiler exit and the boiler stack entrance. Its fitting loss coefficient was calculated as an entrance loss and a cross flow loss stemming from the mixing of the boiler exit and boiler draft diverter air streams. The entrance loss was taken from the ASHRAE Handbook, Table B-1, Section 1.1, page 33.28, with $L/D=0.5$ and $t/D=0$.

$$K_{\text{draft entrance}} = 1.0 \quad C_{l_{\text{draft entrance}}} = 1.0 \quad A_{\text{draft entrance}} = 0.28 \text{ m}^2$$

The cross-flow fitting loss coefficient was taken from the ASHRAE Handbook, Table B-6, Section 6.2, page 33.35, based upon the flow assumptions made in the boiler exit calculation. From these values, we obtained the fitting loss coefficient corresponding to the boiler draft diverter cross flow, and using velocity correction of 1.55 yielded:

$$K_{\text{cross flow}} = 1.53 \quad C_{l_{\text{cross flow}}} = 0.81 \quad A_{\text{cross flow}} = 0.28 \text{ m}^2$$

The total pressure losses for this component are summarized in Table B.5.

Subcomponents	C_l	Area (m ²)	L (m ²)	1/L ²
Entrance	1.0	0.28	0.28	13 (41%)
Cross flow	0.81	0.28	0.23	19 (59%)
Total (effective)			0.18	32 (100%)

Boiler Stack

The boiler stack is a galvanized-steel tube of diameter 0.35 m and total length 0.76 m. Because the ratio l/D is ≤ 7 , frictional losses were ignored. As seen in the Figure B.5, the boiler stack was modeled as three resistances in series:

- A rectangular to round contraction that models the transition from the rectangular boiler draft to the round boiler stack.
- An elbow.
- An elbow exit to the chimney stack.

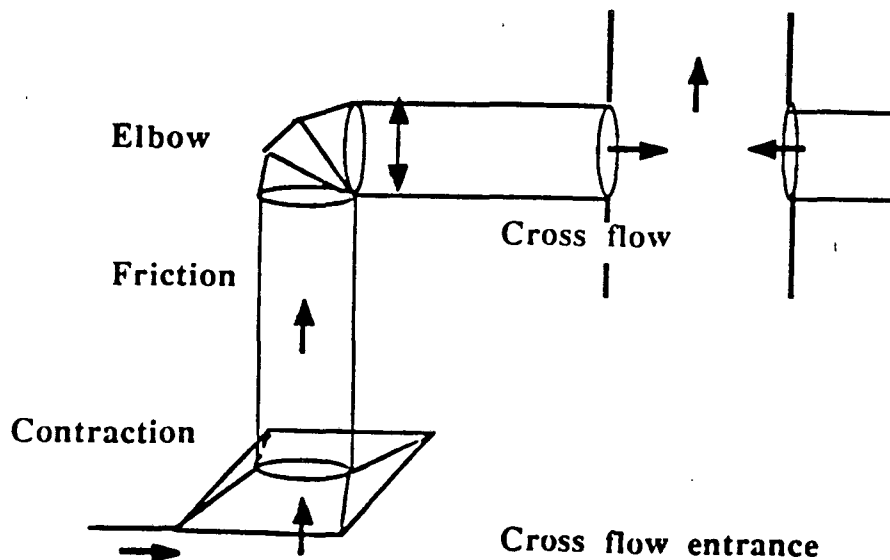


Figure B.5

1. The fitting loss coefficient for the **rectangular to round duct transition** between the draft diverter and the stack can be determined from the ASHRAE Handbook, Table B-5, Section 5.2, page 33.35. The ratio A_0/A_1 is determined as 0.34 from the area of the boiler draft diverter, $A_1=0.28 \text{ m}^2$, and the the area of the stack, $A_0=0.096 \text{ m}^2$. The angle, θ , used was 180 degrees. From these values we obtained:

$$K_{\text{contraction}} = 0.37 \quad C_{l_{\text{contraction}}} = 1.64 \quad A_{\text{contraction}} = 0.096 \text{ m}^2$$

2. The fitting loss coefficient of the **elbow** was obtained from the ASHRAE Handbook, Table B-3, Section 3.2, page 33.31. The 90 degree elbow is made of three pieces and the ratio $r/D=0.5$, resulting in:

$$K_{\text{elbow}} = 0.98 \quad C_{l_{\text{elbow}}} = 1.01 \quad A_{\text{elbow}} = 0.096 \text{ m}^2$$

3. The fitting loss coefficient corresponding to the boiler stack **elbow exit** was taken from the ASHRAE Handbook, Table B-3, Section 3.10, page 33.32. This loss results the 90° transition from the round stack to the square chimney. The values used in Table 3-10 to obtain the fitting loss coefficient were $H_0/W_0=1.0$ and $W_1/W_0=1.2$. The resulting fitting loss coefficient was:

$$K_{\text{exit}} = 1.12 \quad C_{l_{\text{exit}}} = 0.94 \quad A_{\text{exit}} = 0.096 \text{ m}^2$$

The individual losses contributing to the boiler stack fitting loss coefficient are summarized in Table B.6.

Subcomponents	C_l	Area (m^2)	L (m^2)	$1/L^2$
Contraction	1.6	0.096	0.15	44 (16%)
Elbow	1.0	0.096	0.096	110 (40%)
Exit elbow	0.94	0.096	0.090	123 (44%)
Total (effective)			0.060	277 (100%)

Domestic Hot Water Heater

The Domestic Hot Water (DHW) heater was modeled as four resistances in series:

- An entrance partially obstructed by two pipe sections.
- A contraction from the circular entrance to the circular DHW flue.
- The frictional losses in the DHW flue.
- A cross-flow exit.

These resistances are represented in Figure B.6.

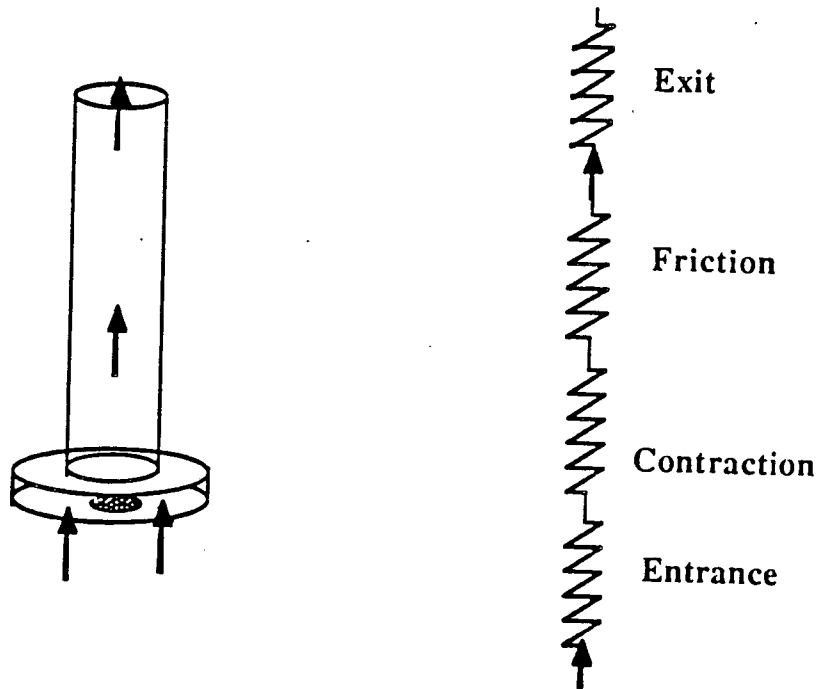


Figure B.6

- **1. The entrance** to the DHW heater is circular (diameter 0.27 m) obstructed by two pipes of 0.06 m diameter. The fitting loss coefficient was estimated by modeling the entrance as a circular pipe partially obstructed by a round butterfly damper. The area obstructed by the damper represents the total area obstructed by the two pipe sections, which resulted in a tilting angle of 20 degrees. The resulting coefficients obtained from the ASHRAE Handbook, Table B-7, Section 7.1, page 33.41, were:

$$K_{\text{entrance}} = 1.5 \quad C_{l_{\text{entrance}}} = 0.82 \quad A_{\text{entrance}} = 0.057 \text{ m}^2$$

2. The **contraction** transition from the entrance diameter to the flue diameter was taken from the ASHRAE Handbook, Table B-5, Section 5.1, page 33.35, using a contraction ratio A_1/A_0 of 3.2 at an angle of 180 degrees. The results were:

$$K_{\text{contraction}} = 0.35 \quad C_{l_{\text{contraction}}} = 1.68 \quad A_{\text{contraction}} = 0.018 \text{ m}^2$$

3. The **frictional losses** were based upon the parameters in Table B.7, using Table 13 on page 4.10 of the ASHRAE Handbook to compute the friction factor.

Table B.7: Friction parameters for DHW flue.	
Inside diameter [m]	D=0.15
Roughness height [m]	$\epsilon=0.00015$
Ratio ϵ/D	0.001
Reynolds number	8000
Friction factor	0.034

The Reynolds number corresponds to a computed flow rate of 75 standard m^3/hr at a temperature of 250°C during DHW firing. During the off-cycle the Reynolds number becomes 11000, which results in a friction factor of 0.032. Using a friction factor of 0.033, a length of 1.44 m, and a diameter of 0.15 m, we then obtained:

$$K_{\text{friction}} = 0.32 \quad C_{l_{\text{friction}}} = 1.78 \quad A_{\text{friction}} = 0.018 \text{ m}^2$$

- 4. The **cross-flow exit** fitting loss coefficient was taken from the ASHRAE Handbook, Table B-6, Section 6.4, page 33.36. This is a very rough approximation of the flow conditions, but no better approximation was available. Using a flow of $75 \text{ m}^3/\text{h}$ through the flue, and $100 \text{ m}^3/\text{h}$ through the draft diverter, the fitting loss coefficient computed was 0.21. To reference this loss coefficient to the flow through the flue it was multiplied by the square of the stack/flue velocity ratio, which yielded:

$$K_{\text{exit}} = 0.59 \quad C_{l_{\text{exit}}} = 1.3 \quad A_{\text{exit}} = 0.018 \text{ m}^2$$

The pressure losses for each subcomponent of the DHW heater are summarized in Table B.8.

Subcomponents	C_l	Area (m^2)	L (m^2)	$1/L^2$
Entrance	0.82	0.057	0.047	453 (10%)
Contraction	1.68	0.018	0.030	1111 (36%)
Friction	1.78	0.018	0.032	976 (22%)
Cross-flow Exit	1.30	0.018	0.023	1821 (42%)
Total (effective)			0.015	4361 (100%)

DHW Draft Diverter

The draft diverter for the DHW heater was modeled as an entrance and a cross-flow connection with the DHW flue. A geometrical description of the draft diverter and the stack is given in Figure B.7. For the entrance we used the ASHRAE Handbook, Table B-1, Section 1.1, page 33.28, with $L/D=0.54$ and $t/D=0.02$, which yields:

$$K_{\text{diverter entr}} = 0.72 \quad C_{l_{\text{diverter entr}}} = 1.18 \quad A_{\text{diverter entr}} = 0.079 \text{ m}^2$$

4. The cross-flow fitting loss coefficient was essentially impossible to determine from the tables in the ASHRAE Handbook. The area ratios corresponding to this fitting are not in the tables, and depending upon with set of ratios were used in Table B-6, Section 6.4, page 33.36, of the ASHRAE Handbook, the loss coefficient could go from positive to negative. As a result a value of zero was chosen for the fitting loss coefficient corresponding to the cross-flow.

DHW Heater Stack

The DHW heater stack is a pipe of inside diameter 0.18 m and of total length 2.4 m. It was modeled as four resistances in series:

- An entrance contraction.
- A frictional loss.
- Two elbows.
- A cross flow exit to the chimney stack.

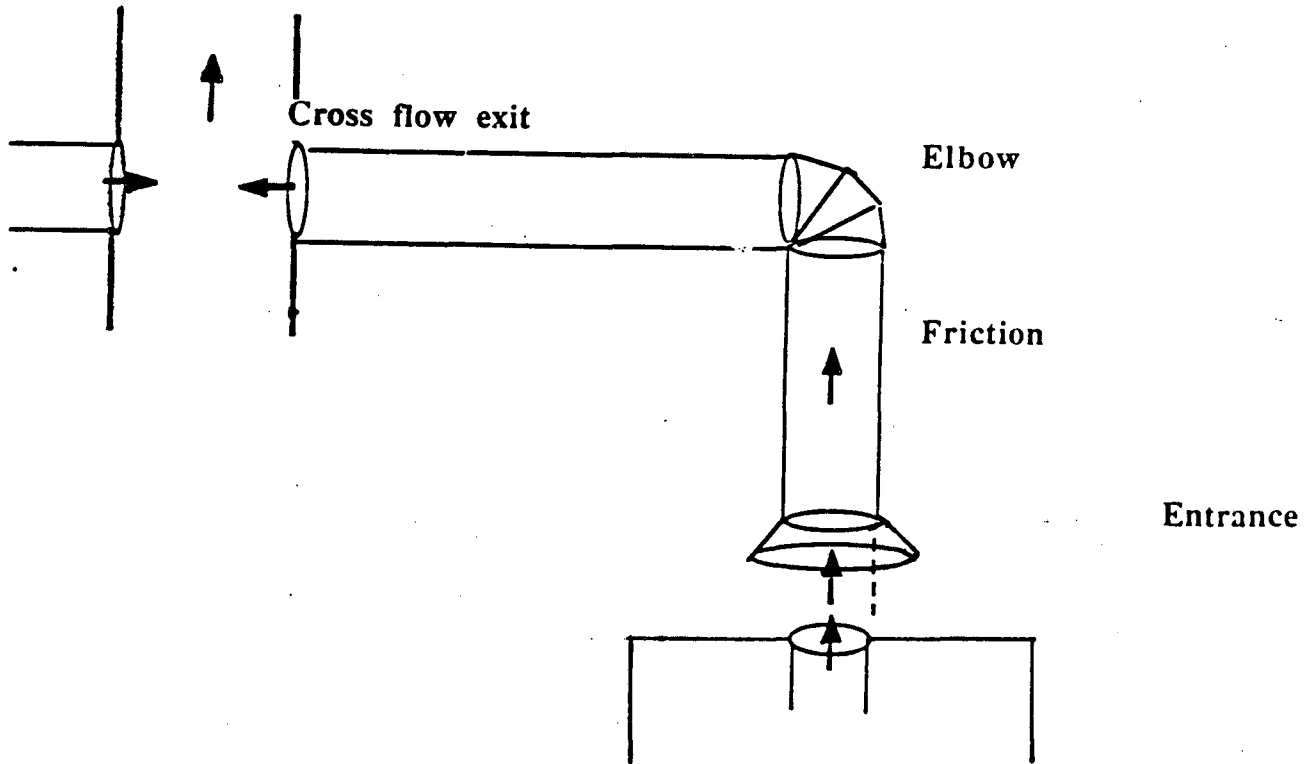


Figure B.7

- **1. The entrance** fitting loss coefficient was computed from the ASHRAE Handbook, Table B-5, Section 5.2, page 33.35. The data required in the table were: $L=0.05$ m and $D=0.18$ m, so that the ratio L/D was 0.27, which along with an angle $\theta=30$ degrees gave:

$$K_{\text{entrance}} = 0.14 \quad C_{l_{\text{entrance}}} = 2.67 \quad A_{\text{entrance}} = 0.025 \text{ m}^2$$

- 2. The frictional losses were computed from the parameters in Table B.9.

Table B.9: Friction Parameters for the DHW Heater Stack	
Inside diameter [m]	D=0.18
Length of the pipe [m]	L=2.4
Roughness height [m]	$\epsilon=0.00015$
Ratio ϵ/D	0.00083
Reynolds number	23000
Friction factor	0.028

The Reynolds number was obtained from a measured flow rate of 175 standard m^3/h at a temperature of 100°C . From these data, we obtained:

$$K_{\text{friction}} = 0.37 \quad C_{l_{\text{friction}}} = 1.64 \quad A_{\text{friction}} = 0.025 \text{ m}^2$$

- 3. The elbow fitting loss coefficients were computed from the ASHRAE Handbook, Table B-3, page 33.31, Section 3.2. We assumed a three-piece 90 degree elbow with a ratio $r/D=0.75$, which resulted in:

$$K_{\text{elbow}} = 0.54 \quad C_{l_{\text{elbow}}} = 1.36 \quad A_{\text{elbow}} = 0.025 \text{ m}^2$$

- 4. The cross flow exit fitting loss coefficient was essentially impossible to determine from the ASHRAE Handbook. None of the sections in Table B-6 fit exactly the situation in the DHW-stack/chimney; depending upon which compromise was made the value varied from 0.40 to -0.56. For this reason, the pressure loss was assumed to be zero in this instance.

The different calculations used for computing the DHW stack fitting loss coefficient are summarized in the following: The pressure losses for each subcomponent of the

DHW heater stack are summarized in Table B.10.

Subcomponents	C_l	Area (m^2)	L (m^2)	$1/L^2$
Entrance	2.67	0.025	0.067	224 (9%)
Friction	1.64	0.025	0.041	595 (23%)
Elbow one	1.36	0.025	0.034	865 (34%)
Elbow two	1.36	0.025	0.034	865 (34%)
Cross-flow Exit	n/a	n/a	n/a	n/a
Total (effective)			0.020	2549 (100%)

Chimney

The chimney was modeled as two resistances in series as shown in Figure B.8, representing the frictional losses and the dynamic losses at the exit.

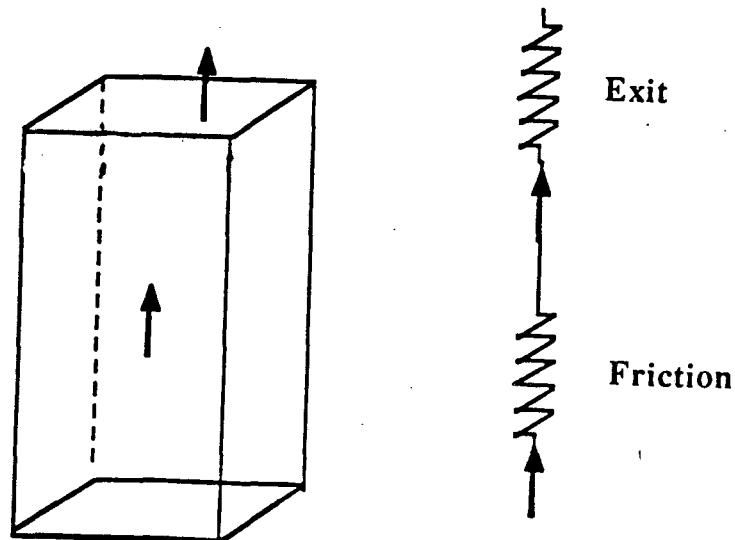


Figure B.8

1. The frictional loss fitting coefficient was computed from the values in Table B.11.

Hydraulic diameter [m]	D=0.38
Length of the chimney [m]	L=12.2
Roughness height [m]	$\epsilon=0.0015$
Ratio ϵ/D	0.004
Reynolds number	44000
Friction factor	0.031

The roughness height in Table B.11 was taken from the ASHRAE Handbook of Fundamentals for clay pipe.¹⁴ The Reynolds number was obtained from a measured flow rate of 1000 standard m³/hr, at a temperature of 60°C. From these data, we obtained:

$$K_{\text{friction}} = 1.0 \quad C_{\text{friction}} = 1.0 \quad A_{\text{friction}} = 0.14 \text{ m}^2$$

2. The exit loss coefficient is taken from the ASHRAE Handbook, Table B-2, Section 2.1, page 33.29:

$$K_{\text{exit}} = 1.0 \quad C_{\text{entrance}} = 1.0 \quad A_{\text{entrance}} = 0.144 \text{ m}^2$$

The individual losses contributing to the chimney fitting loss coefficient are summarized in Table B.12.

Subcomponents	C_l	Area (m ²)	L (m ²)	1/L ²
Friction	1.0	0.14	0.14	51 (50%)
Exit	1.0	0.144	0.14	51 (50%)
Total (effective)			0.099	102 (100%)

Summary of the Leakage Area Calculations

Table B.13: Boiler Components Leakage Areas				
Subcomponents	C_1	Area (m ²)	L (m ²)	1/L ²
Entrance	1.4	0.10	0.14	51 (15%)
Diffuser-elbow	1.1	0.10	0.11	83 (24%)
Heat exchanger	0.59	0.13	0.077	169 (49%)
Elbow	0.58	0.81	0.47	5 (1%)
Exit contraction	1.8	0.13	0.23	19 (5%)
Exit cross flow	1.8	0.13	0.23	19 (5%)
Total boiler flue			0.054	346
Entrance	1.0	0.28	0.28	13 (41%)
Cross flow	0.81	0.28	0.23	19 (59%)
Total boiler draft			0.18	32
Contraction	1.6	0.096	0.15	44 (16%)
Elbow	1.0	0.096	0.096	110 (40%)
Exit elbow	0.94	0.096	0.090	123 (44%)
Total boiler stack			0.060	277

Table B.14: DHW Heater Components and Chimney Leakage Areas				
Subcomponents	C_l	Area (m^2)	L (m^2)	$1/L^2$
Entrance	0.82	0.057	0.047	453 (10%)
Contraction	1.68	0.018	0.030	1111 (36%)
Friction	1.78	0.018	0.032	976 (22%)
Cross-flow Exit	1.30	0.018	0.023	1821 (42%)
Total DHW flue			0.015	4361
Total DHW draft	1.18	0.079	0.093	115
Entrance	2.67	0.025	0.067	224 (9%)
Friction	1.64	0.025	0.041	595 (23%)
Elbow one	1.36	0.025	0.034	865 (34%)
Elbow two	1.36	0.025	0.034	865 (34%)
Cross-flow Exit	n/a	n/a	n/a	n/a
Total DHW stack			0.020	2549
Friction	1.0	0.14	0.14	51 (50%)
Exit	1.0	0.14	0.14	51 (50%)
Total Chimney			0.099	102

The percentages in Tables B.13 and B.14 indicate the relative importance of the resistance of each subcomponent. This information can be used to simplify the calculations by neglecting the resistances which are less than 10 percent of the total resistance value. For example, the elbow and the exit of the boiler flue could probably be neglected.

Modeling a Damper

Geometric description

The damper that would most likely be installed in our example system would be a circular damper located in the boiler stack. These dampers typically do not seal perfectly, and are often fitted with a small cutout on systems with a pilot. For our example we chose a diameter of 33.5 cm, 1.5 cm less than the boiler stack diameter, and included a circular cutout of diameter 4 cm.

Modeling methods

The damper was modeled as two resistances in parallel resulting from the superposition of an orifice and a circular damper. This approximation is shown in Figure B.9.

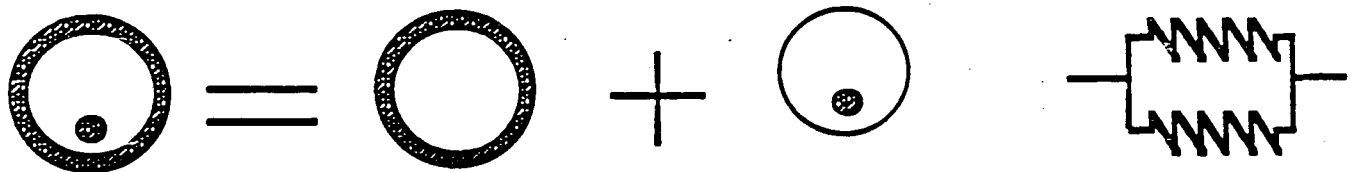


Figure B.9

The fitting loss coefficient for the cutout (orifice) can be approximated from the pressure loss across an orifice plate flow meter. The equation for such a loss, referenced to the orifice area (from E. Ower, R.C. Prankhurst, *The measurement of air flow*, Pergamon Press, 1977, page 170), is:

$$K_{\text{orifice}} = \frac{1}{0.606^2} \left(1 - \left(\frac{A_{\text{hole}}}{A_{\text{duct}}} \right)^2 \right) \left(1 - \frac{A_{\text{hole}}}{A_{\text{duct}}} \right)$$

For the cutout in the damper modeled for the Bosworth building the result is:

$$K_{\text{cutout}} = 2.67 \quad C_{l_{\text{cutout}}} = 0.61 \quad A_{\text{cutout}} = 0.0013 \text{ m}^2$$

The damper was modeled as a rectangular damper gate, for which data are available in the ASHRAE Handbook, Table B-7, Section 7.4, page 33.42. The analogy is described in Figure B.10. The gap to opening height ratio in the ASHRAE handbook is equivalent to our gap area to duct area ratio, which for a 0.75 cm gap is 0.084. Because this value is

lower than any of the tabulated values, extrapolation was necessary. A model of the form $K = e^{-bx}$, with $x=h/H$, was found to fit the data very well. Substituting our ratio of 0.084 for x the resulting fitting loss coefficient was:

$$K_{\text{gap}} = 0.57 \quad C_{l_{\text{gap}}} = 1.33 \quad A_{\text{gap}} = 0.0081 \text{ m}^2$$

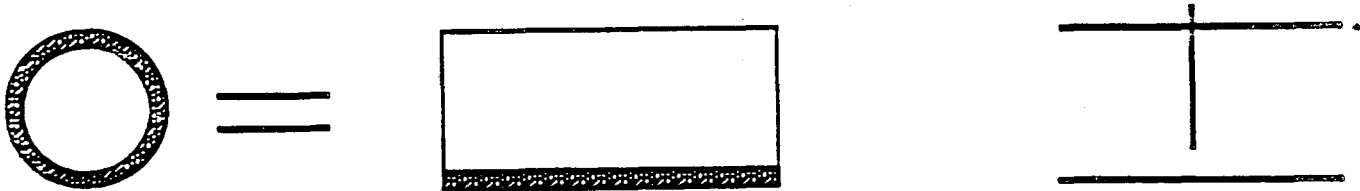


Figure B.10

The leakage of the vent damper, and the leakage of the boiler stack with and without the vent damper are presented in Table B.15.

Table B.15: Summary of Leakage Areas of Vent Damper and Boiler Stack				
Subcomponents	C_l	Area (m^2)	L (m^2)	$1/L^2$
Cutout	0.61	0.0013	0.00079 (7%)	1.6×10^6
Gap	1.33	0.0081	0.011 (93%)	8616
Total Vent Damper			0.012 (100%)	6944
Boiler Stack w/o VD			0.060	277
Boiler Stack w VD			0.012	7221

APPENDIX C

REDUCTION OF THE SYSTEM OF EQUATIONS

Summary of Equations and Unknowns

In the main body of the report we developed a system of 18 equations and 18 unknowns, which are summarized as follows:

Unknowns:

Table C.1 Summary of Unknowns		
Temperatures	Pressures	Mass flows
T_b	P_{br}	m_b
T_{bs}	P_b	m_{bd}
T_d	P_d	m_{bs}
T_{ds}	P_s	m_d
T_{cb}		m_{dd}
T_{cm}		m_{ds}
		m_s
		m_{br}

Equations:

The following equations are the same as those described in the main body of the report. As mentioned in the main body, the outside pressure is taken as the reference pressure, so that $P_{out} = 0$.

$$m_{bs} = m_b + m_{bd} \quad [14]$$

$$m_{ds} = m_d + m_{dd} \quad [15]$$

$$m_s = m_b + m_{bd} + m_d + m_{dd} \quad [16]$$

$$m_{br} = m_s \quad [17]$$

$$m_b C_{p_{air}} (T_b - T_{br}) = Q_{l_b} \quad [18]$$

$$m_d C_{p_{air}} (T_d - T_{br}) = Q_{l_d} \quad [19]$$

$$m_{bs} T_{bs} = m_b T_b + m_{bd} T_{br} \quad [20]$$

$$m_{ds} T_{ds} = m_d T_d + m_{dd} T_{br} \quad [21]$$

$$m_s T_{cb} = m_{bs} T_{bs} + m_{ds} T_{ds} \quad [22]$$

$$0 - P_{br} = \frac{1}{2\rho_{out}} \left(\frac{m_{br}}{L_{br}} \right)^2 \quad [23]$$

$$P_{br} - P_b = \frac{1}{2\rho_{br}} \left(\frac{m_{bd}}{L_{bd}} \right)^2 \quad [24]$$

$$P_{br} - P_d = \frac{1}{2\rho_{br}} \left(\frac{m_{dd}}{L_{dd}} \right)^2 \quad [25]$$

$$P_{br} - P_b - (\rho_b - \rho_{br}) g h_b = \frac{1}{2\rho_b} \left(\frac{m_b}{L_b} \right)^2 \quad [26]$$

$$P_{br} - P_d - (\rho_d - \rho_{br}) g h_d = \frac{1}{2\rho_d} \left(\frac{m_d}{L_d} \right)^2 \quad [27]$$

$$P_b - P_s = \frac{1}{2\rho_{bs}} \left(\frac{m_{bs}}{L_{bs}} \right)^2 \quad [28]$$

$$P_d - P_s = \frac{1}{2\rho_{ds}} \left(\frac{m_{ds}}{L_{ds}} \right)^2 \quad [29]$$

$$P_s - 0 - (\rho_{cm} - \rho_{out}) g h_s = \frac{1}{2\rho_{cm}} \left(\frac{m_s}{L_s} \right)^2 \quad [30]$$

$$T_c(z+\Delta z, t) = T_c(z, t) \left(1 - \frac{\Delta z}{\lambda_z}\right) + \frac{\Delta z}{\lambda_z} T_{brick}(z, t) \quad [48]$$

$$T_{brick}(x, t+\Delta t) = \frac{\Delta t}{\lambda_t} T_c(z, t) + R_U \frac{\Delta t}{\lambda_t} T_{amb} + (1 - (1+R_U) \frac{\Delta t}{\lambda_t}) T_{brick}(z, t) \quad [49]$$

Reduction from 18 unknowns to 4 unknowns

The two equations [48] and [49] are used to obtain the temperature profile inside the chimney, then to deduce the unknown: T_{cm} .

The four unknowns that we will keep in the reduction are m_b , m_d , m_{bd} and m_{dd} . The other unknowns can be expressed with respect to these unknowns with relatively

straightforward expressions.

- m_{bs} is deduced directly from equation [14]:

$$m_{bs} = m_b + m_{bd} \quad [C.1]$$

- m_{ds} is deduced directly from equation [15]:

$$m_{ds} = m_d + m_{dd} \quad [C.2]$$

- m_s is deduced from equations [C.1], [C.2] and [16]:

$$m_s = m_b + m_{bd} + m_d + m_{dd} \quad [C.3]$$

- From equation [18], we deduce T_b :

$$T_b = \frac{Q_{lb}}{C_{p_{air}} m_b} + T_{br} \quad [C.4]$$

- From equation [19], we deduce T_d :

$$T_d = \frac{Q_{ld}}{C_{p_{air}} m_d} + T_{br} \quad [C.5]$$

- From equations [20], [14], and [C.4], we obtain:

$$T_{bs} = \frac{Q_{lb}}{C_{p_{air}} (m_b + m_{bd})} + T_{br} \quad [C.6]$$

- From equations [21], [15], and [C.5], we obtain:

$$T_{ds} = \frac{Q_{ld}}{C_{p_{air}} (m_d + m_{dd})} + T_{br} \quad [C.7]$$

- From equations [22], [C.3], [C.6] and [C.7], we obtain:

$$T_{cb} = \frac{Q_{lb} + Q_{ld}}{C_{p_{air}} (m_b + m_{bd} + m_d + m_{dd})} + T_{br} \quad [C.8]$$

• From equation [23] and [17], we obtain P_{br} :

$$P_{br} = -\frac{1}{2\rho_{out}} \left(\frac{m_s}{L_{br}} \right)^2 \quad [C.9]$$

• From equation [24], we obtain P_b :

$$P_b = -\frac{1}{2\rho_{br}} \left(\frac{m_{bd}}{L_{bd}} \right)^2 - \frac{1}{2\rho_{out}} \left(\frac{m_s}{L_{br}} \right)^2 \quad [C.10]$$

• From equation [25], we obtain P_d :

$$P_d = -\frac{1}{2\rho_{br}} \left(\frac{m_{dd}}{L_{dd}} \right)^2 - \frac{1}{2\rho_{out}} \left(\frac{m_s}{L_{br}} \right)^2 \quad [C.11]$$

• From equation [28], we obtain P_s :

$$P_s = -\frac{1}{2\rho_{br}} \left(\frac{m_{bd}}{L_{bd}} \right)^2 - \frac{1}{2\rho_{out}} \left(\frac{m_s}{L_{br}} \right)^2 - \frac{1}{2\rho_{bs}} \left(\frac{m_b + m_{bd}}{L_{bs}} \right)^2 \quad [C.12]$$

All the coefficients a_i are described at the end of this appendix. They have been used to simplify the presentation of the equations. The reader will also notice that we sometimes kept m_s in some of these equations to shorten the presentation; m_s should always be replaced by [C.3].

• Eliminating P_{br} and P_d by substituting Equation 25 into Equation 27, and using [C.5] and the ideal gas law to eliminate ρ_d , by rearranging the terms we obtain:

$$a_{24}m_d^3 + 2a_1m_d^2 + a_2m_d - a_{25}m_{dd}^2m_d - a_3m_{dd}^2 - a_4 = 0 \quad [50]$$

• Eliminating P_{br} and P_b by substituting Equation 24 into Equation 26, and using [C.4] and the ideal gas law to eliminate ρ_b , by rearranging the terms we obtain:

$$a_{26}m_b^3 + 2a_{12}m_b^2 + a_{13}m_b - a_{27}m_bm_{bd}^2 - a_{14}m_{bd}^2 - a_{15} = 0 \quad [52]$$

• If we now replace P_s and P_d in Equation 29 by [C.12] and [C.11] and eliminate ρ_{ds} using [C.7] and the ideal gas law, we obtain:

$$\begin{aligned}
& a_6 m_{bd}^2 - a_7 m_{dd}^2 + a_8 (m_b + m_{bd})^2 + a_9 (m_b + m_{bd}) \\
& = a_{10} (m_d + m_{dd})^2 + a_{11} (m_d + m_{dd})
\end{aligned} \tag{51}$$

• Finally, if we replace P_s by [C.12] in [30] and use [C.6] plus the ideal gas law to eliminate ρ_{bs} we obtain:

$$a_{23} m_s^2 + a_{18} m_{bd}^2 + a_{21} (m_b + m_{bd})^2 + a_{22} (m_b + m_{bd}) - a_{20} = 0 \tag{53}$$

The discussion of these four equations and the method chosen to solve them is presented in the main body of the report.

Description of the Coefficients a_i

In these expressions, T_{br} is the boiler room temperature in degrees Kelvin, T_{out} is the outside temperature in degrees Kelvin, L_i is the leakage area corresponding to the component i of the heating system, and g is the acceleration of gravity.

$$a_1 = \frac{1}{2 * \rho_{br} L_d^2}$$

$$a_2 = \frac{Q_{ld}}{2 * \rho_{br} L_d^2}$$

$$a_3 = \frac{1}{2 * \rho_{br} L_{dd}^2}$$

$$a_4 = \rho_{br} g h_d$$

$$a_5 = \frac{a_1}{a_2}$$

$$a_6 = \frac{1}{2 * \rho_{br} L_{bd}^2}$$

$$a_7 = \frac{1}{2 * \rho_{br} L_{dd}^2}$$

$$a_8 = \frac{1}{2 * \rho_{br} L_{bs}^2}$$

$$a_9 = \frac{Q_{lb}}{2 * \rho_{br} L_{bs}^2}$$

$$a_{10} = \frac{1}{2 * \rho_{br} L_{ds}^2}$$

$$a_{11} = \frac{Q_{ld}}{2 * \rho_{br} L_{ds}^2}$$

$$a_{12} = \frac{1}{2 * \rho_{br} L_b^2}$$

$$a_{13} = \frac{Q_{lb}}{2 * \rho_{br} L_b^2}$$

$$a_{14} = \frac{1}{2 * \rho_{br} L_{bd}^2}$$

$$a_{15} = \rho_{br} g h_b$$

$$a_{16} = \frac{a_{12}}{a_{13}}$$

$$a_{17} = \frac{1}{2 \rho_{out} L_{br}^2}$$

$$a_{18} = \frac{1}{2 \rho_{br} L_{bd}^2}$$

$$a_{19} = \frac{1}{2 \rho_{cm} L_s^2}$$

$$a_{20} = -g h_s (\rho_{cm} - \rho_{out})$$

$$a_{21} = \frac{1}{2 \rho_{br} L_{bs}^2}$$

$$a_{22} = \frac{Q_{lb}}{2 \rho_{br} L_{bs}^2}$$

$$a_{23} = a_{19} + a_{17}$$

$$a_{24} = \frac{a_1^2}{a_2}$$

$$a_{25} = \frac{a_1 a_3}{a_2}$$

$$a_{26} = \frac{a_{12}^2}{a_{13}}$$

$$a_{27} = \frac{a_{12} a_{14}}{a_{13}}$$

$$a_{28} = a_{24} - a_{25}$$

APPENDIX D

INPUT AND OUTPUT DATA FOR 6-UNIT APARTMENT BUILDING

You will find in the following an example of the input to and the output from the vent system simulation program for the venting system of a 6-unit apartment building in Chicago, IL.

 * Bosworth boiler input *

* Leakage areas *

* Leakage area of chimney : 990.0 cm2
 * Leakage area of boiler stack
 without damper : 600.0 cm2
 with damper : 600.0 cm2
 * Leakage area of DHW stack
 without damper : 200.0 cm2
 with damper : 200.0 cm2
 * Leakage area of boiler : 540.0 cm2
 * Leakage area of DHW : 150.0 cm2
 * Leakage area of boiler draft diverter: 1800.0 cm2
 * Leakage area of DHW draft diverter : 930.0 cm2
 * Leakage area of boiler room : 2500.0 cm2

* Physical Characteristics *

* Width of the chimney : 35.0 cm
 * Width of the brick : 21.0 cm

 * Height of chimney : 12.2 m
 * Height of boiler : 1.5 m
 * Height of DHW : 1.5 m

* Temperatures *

* Temperature of boiler room : 24.0 deg c
 * Temperature outside : 0.0 deg c
 * Temperature of the ambient : 20.0 deg c
 * Temperature of the boiler water : 100.0 deg c
 * Temperature of the dhw water : 50.0 deg c

* Thermal Characteristics *

* Efficiency of the boiler : 0.85
 * Efficiency of the DHW : 0.85

 * Energy input in the boiler : 1.0 Mbtu/hr
 * Boiler time constant ON : 4.0 minutes
 * Boiler time constant OFF : 720.0 minutes

 * Energy input in the DHW : 0.2 Mbtu/hr
 * DHW time constant ON : 3.0 minutes
 * DHW time constant OFF : 360.0 minutes

* Cycle information *

* The boiler is cycling : ON at : 2 minutes
 * The boiler is cycling : OFF at : 22 minutes
 * The boiler is cycling : ON at : 42 minutes

* The boiler is cycling	:OFF	at	:	48	minutes
* The boiler is cycling	: ON	at	:	54	minutes
* The boiler is cycling	:OFF	at	:	60	minutes
* The dhw is cycling	: ON	at	:	20	minutes
* The dhw is cycling	:OFF	at	:	25	minutes
* The dhw is cycling	: ON	at	:	30	minutes
* The dhw is cycling	:OFF	at	:	35	minutes
* The dhw is cycling	: ON	at	:	40	minutes
* The dhw is cycling	:OFF	at	:	60	minutes
* Time limit for the study			:	60	minutes
* Interval of time for the study			:	60	seconds

* Discretisation data *

* Number of points taken in the chimney:	15	points
* Maximal error in the iteration	:	0.002

 * Bosworth boiler/off output *

 * Time : 0 minute *

***** Flow rates *****			***** Ratios *****	
	Local	Room		
	density	density		
* Boiler flue :	563.3	440.6 m3/hr	* * mb/mbs=0.45*	*
* Boiler draft:	555.3	545.5 m3/hr	* *	*
* Boiler stack:	1118.7	986.1 m3/hr	* *	*
* DHW flue :	93.3	84.3 m3/hr	* * md/mds=0.30*	*
* DHW draft :	204.3	200.7 m3/hr	* *	*
* DHW stack :	297.7	285.0 m3/hr	* *	*
* Total stack :	1416.3	1271.1 m3/hr	* * mbs/ms=0.78*	*

 * Temperatures *

* Boiler room	:	24.0 deg c	*
* Boiler flue	:	100.0 deg c	*
* DHW flue	:	50.1 deg c	*
* Boiler stack	:	58.0 deg c	*
* DHW stack	:	31.7 deg c	*
* Stack bottom	:	52.1 deg c	*
* Stack top	:	50.1 deg c	*

 * Pressures referenced to outside [Pa] *

* pbr=	-1.1	pb=	-2.9	pd=	-1.4	ps=	-17.2	*
--------	------	-----	------	-----	------	-----	-------	---

 * Time : 3 minute *

 * Flow rates * * Ratios *

 * Local Room * *
 * density density * *
 * Boiler flue : 676.9 482.9 m3/hr * * mb/mbs=0.46*
 * Boiler draft: 570.7 560.6 m3/hr * * *
 * Boiler stack: 1247.7 1043.5 m3/hr * * *
 * DHW flue : 95.0 86.1 m3/hr * * md/mds=0.26*
 * DHW draft : 254.2 249.7 m3/hr * * *
 * DHW stack : 349.2 335.8 m3/hr * * *
 * Total stack : 1596.9 1379.3 m3/hr * * mbs/ms=0.76*

 * Temperatures *

 * Boiler room : 24.0 deg c *
 * Boiler flue : 136.0 deg c *
 * DHW flue : 48.9 deg c *
 * Boiler stack : 75.8 deg c *
 * DHW stack : 30.4 deg c *
 * Stack bottom : 64.8 deg c *
 * Stack top : 61.6 deg c *

 * Pressures referenced to outside [Pa] *

 * pbr= -1.3 pb= -3.2 pd= -1.8 ps=-20.1 *

 * Time : 5 minute *

 * Flow rates * * Ratios *

 * Local Room * * *
 * density density * * *
 * Boiler flue : 807.3 514.2 m3/hr * * mb/mbs=0.46*
 * Boiler draft: 604.3 593.6 m3/hr * * *
 * Boiler stack: 1411.6 1107.8 m3/hr * * *
 * DHW flue : 97.6 88.4 m3/hr * * md/mds=0.24*
 * DHW draft : 285.3 280.3 m3/hr * * *
 * DHW stack : 382.9 368.7 m3/hr * * *
 * Total stack : 1794.5 1476.5 m3/hr * * mbs/ms=0.75*

 * Temperatures *

 * Boiler room : 24.0 deg c *
 * Boiler flue : 185.0 deg c *
 * DHW flue : 49.0 deg c *
 * Boiler stack : 98.7 deg c *
 * DHW stack : 30.0 deg c *
 * Stack bottom : 81.6 deg c *
 * Stack top : 77.1 deg c *

 * Pressures referenced to outside [Pa] *

 * pbr= -1.5 pb= -3.6 pd= -2.1 ps=-23.9 *

 * Time : 6 minute *

 * Flow rates * * Ratios *

 * Local Room * *
 * density density * *
 * Boiler flue : 847.5 520.7 m3/hr * * mb/mbs=0.46*
 * Boiler draft: 613.2 602.3 m3/hr * *
 * Boiler stack: 1460.7 1123.0 m3/hr * *
 * DHW flue : 98.5 89.3 m3/hr * * md/mds=0.23*
 * DHW draft : 297.8 292.5 m3/hr * *
 * DHW stack : 396.3 381.8 m3/hr * *
 * Total stack : 1857.0 1504.8 m3/hr * * mbs/ms=0.75*

 * Temperatures *

 * Boiler room : 24.0 deg c *
 * Boiler flue : 201.8 deg c *
 * DHW flue : 48.9 deg c *
 * Boiler stack : 106.5 deg c *
 * DHW stack : 29.8 deg c *
 * Stack bottom : 87.0 deg c *
 * Stack top : 82.0 deg c *

 * Pressures referenced to outside [Pa] *

 * pbr= -1.6 pb= -3.7 pd= -2.2 ps=-25.0 *

LAWRENCE BERKELEY LABORATORY
TECHNICAL INFORMATION DEPARTMENT
1 CYCLOTRON ROAD
BERKELEY, CALIFORNIA 94720